References

Bédard A, Parent A (2004) Evidence of newly generated neurons in the human olfactory bulb. Brain Res Dev Brain Res 151: 159-168

Brogiolo W, Stocker S, Ikeya T, Rintelen F, Fernandez R, Hafen E (2001) An evolutionarily conserved function of the *Drosophila* insulin receptor and insulin-like peptides in growth control. Curr Biol 11: 213-221

Carson MJ, Behringer RR, Brinster RL, McMorris FA (1993) Insulin-like growth factor I increases brain growth and central nervous system myelination in transgenic mice. Neuron 10: 729-740

Cheng B, Mattson MP (1992) IGF-I and IGF-II protect cultured hippocampal and septal neurons against calcium-mediated hypoglycemic damage. J Neurosci 12: 1558-1586

Curtis MA, Kam M, Nannmark U, Anderson MF, Axell MZ, Wikkelso C, Holtås S, van Roon-Mom WM, Björk-Eriksson T, Nordborg C, *et al* (2007) Human neuroblasts migrate to the olfactory bulb via a lateral ventricular extension. Science 315: 1243-1249

D'Amour KA, Gage FH (2003) Genetic and functional differences between multipotent neural and pluripotent embryonic stem cells. Proc Natl Acad Sci USA 100: 11866-11872

Dictus C, Tronnier V, Unterberg A, Herold-Mende C (2007) Comparative analysis of *in vitro* conditions for rat adult neural progenitor cells. J Neurosci Methods 161: 250-258

Doré S, Kar S, Quirion R (1997) Insulin-like growth factor I protects and rescues hippocampal neurons against beta-amyloid- and human amylin-induced toxicity. Proc Natl Acad Sci USA 94: 4772-4777

Edlund H (2002) Pancreatic organogenesis-developmental mechanisms and implications for therapy. Nat Rev Genet 3: 524-532

Firth SM, Baxter RC (2002) Cellular actions of the insulin-like growth factor binding proteins. Endocrinol Rev 23: 824-825

Gage FH (2000) Mammalian neural stem cells. Science 287: 1433-1438

Gage FH, Coates PW, Palmer TD, Kuhn HG, Fisher LJ, Suhonen JO, Peterson DA, Suhr ST, Ray J (1995) Survival and differentiation of adult neuronal progenitor cells transplanted to the adult brain. Proc Natl Acad Sci USA 92: 11879-11883

Gao Z, Ure K, Ables JL, Lagace DC, Nave KA, Goebbels S, Eisch AJ, Hsieh J (2009) Neurod1 is essential for the survival and maturation of adult-born neurons. Nat Neurosci 12: 1090-1092

Greenwood CE, Winocur G (2005) High-fat diets, insulin resistance and declining cognitive function. Neurobiol Aging 26: 45

Gritti A, Bonfanti L, Doetsch F, Caille I, Alvarez-Buylla A, Lim DA, Galli R, Verdugo JM, Herrera DG, Vescovi AL (2002) Multipotent neural stem cells reside into the rostral extension and olfactory bulb of adult rodents. J Neurosci 22: 437-445

Habener JF, Kemp DM, Thomas MK (2005) Minireview: transcriptional regulation in pancreatic development. Endocrinology 146: 1025-1034

Hayakawa H, Hayashita-Kinoh H, Nihira T, Seki T, Mizuno Y, Mochizuki H (2007) The isolation of neural stem cells from the olfactory bulb of Parkinson's disease model. Neurosci Res 57: 393-398

Hori Y, Gu X, Xie X, Kim SK (2005) Differentiation of insulin-producing cells from human neural progenitor cells. PLoS Med 2: 347-356

Hsieh J, Aimone JB, Kaspar BK, Kuwabara T, Nakashima K, Gage FH (2004) IGF-I instructs multipotent adult neural progenitor cells to become oligodendrocytes. J Cell Biol 164: 111-122

Jessberger S, Clark RE, Broadbent NJ, Clemenson GD, Jr, Consiglio A, Lie DC, Squire LR, Gage FH (2009) Dentate gyrus-specific knockdown of adult neurogenesis impairs spatial and object recognition memory in adult rats. Learn Mem 16: 147-154

Kawaguchi Y, Cooper B, Gannon M, Ray M, MacDonald RJ, Wright CV (2002) The role of the transcriptional regulator Ptf1a in converting intestinal to pancreatic progenitors. Nat Genet 32: 128-134

Kuwabara T, Hsieh J, Muotri A, Yeo G, Warashina M, Lie DC, Moore L, Nakashima K, Asashima M, Gage FH (2009) Wnt-mediated activation of NeuroD1 and retro-elements during adult neurogenesis. Nat Neurosci 12: 1097-1105

Le Roith D (2003) The insulin-like growth factor system. Exp Diabesity Res 4: 205-212

Lee SM, Tole S, Grove E, McMahon AP (2000) A local Wnt-3a signal is required for development of the mammalian hippocampus. Development 127: 457-467

Lie DC, Colamarino SA, Song HJ, Désiré L, Mira H, Consiglio A, Lein ES, Jessberger S, Lansford H, Dearie AR, *et al* (2005) Wnt signalling regulates adult hippocampal neurogenesis. Nature 437: 1370-1375

Lindholm D, Carroll P, Tzimagiogis G, Thoenen H (1996) Autocrine–paracrine regulation of hippocampal neuron survival by IGF-1 and the neurotrophins BDNF, NT-3 and NT-4. Eur J Neurosci 8: 1452-1460

Liu JL (2007) Does IGF-I stimulate pancreatic islet cell growth? Cell Biochem Biophys 48: 115-125

Liu Z, Martin LJ (2003) Olfactory bulb core is a rich source of neural progenitor and stem cells in adult rodent and human. J Comp Neurol 459: 368-391

Liu M, Pleasure SJ, Collins AE, Noebels JL, Naya FJ, Tsai MJ, Lowenstein DH (2000) Loss of BETA2/NeuroD leads to malformation of the dentate gyrus and epilepsy. Proc Natl Acad Sci USA 97: 865-870

Lumelsky N, Blondel O, Laeng P, Velasco I, Ravin R, McKay R (2001) Differentiation of embryonic stem cells to insulin-secreting structures similar to pancreatic islets. Science 292: 1389-1394

McMorris FA, Dubois-Delcq M (1986) Insulin-like growth factor I promotes cell proliferation and oligodendroglial commitment in rat glial progenitor cells developing *in vitro*. J Neurosci Res 21: 199-209

Melloul D, Marshak S, Cerasi E (2002) Regulation of insulin gene transcription. Diabetologia 45: 309-326

Messier C (2005) Impact of impaired glucose tolerance and type 2 diabetes on cognitive aging. Neurobiol Aging 26: S26-S30

Miyata T, Maeda T, Lee JE (1999) NeuroD is required for differentiation of the granule cells in the cerebellum and hippocampus. Genes Dev 13: 1647-1652

Nakashima K, Yanagisawa M, Arakawa H, Kimura N, Hisatsune T, Kawabata M, Miyazono K, Taga T (1999) Synergistic signaling in fetal brain by STAT3-Smad1 complex bridged by p300. Science 284: 479-482

Namihira M, Kohyama J, Semi K, Sanosaka T, Deneen B, Taga T, Nakashima K (2009) Committed neuronal precursors confer astrocytic potential on residual neural precursor cells. Dev Cell 16: 245-255

Naya FJ, Stellrecht CMM, Tsai MJ (1995) Tissue specific regulation of the insulin gene by a novel basic helix loop helix transcription factor. Genes Dev 9: 1009-1019

Naya FJ, Huang HP, Qiu Y, Mutoh H, DeMayo FJ, Leiter AB, Tsai MJ (1997) Diabetes, defective pancreatic morphogenesis, and abnormal enteroendocrine differentiation in BETA2/neuroD-deficient mice. Genes Dev 11: 2323-2334

Nishimura W, Kondo T, Salameh T, El Khattabi I, Dodge R, Bonner-Weir S, Sharma A (2006) A switch from MafB to MafA expression accompanies differentiation to pancreatic beta-cells. Dev Biol 293: 526-539

Pagano SF, Impagnatiello F, Girelli M, Cova L, Grioni E, Onofri M, Cavallaro M, Etteri S, Vitello F, Giombini S, *et al* (2000) Isolation and characterization of neural stem cells from the adult human olfactory bulb. Stem Cells 18: 295-300

Rulifson EJ, Kim SK, Nusse R (2002) Ablation of insulin-producing neurons in flies: growth and diabetic phenotypes. Science 296: 1118-1120

Sander M, German MS (1997) The beta cell transcription factors and development of the pancreas. J Mol Med 75: 327-340

Seaberg RM, Smukler SR, Kieffer TJ, Enikolopov G, Asghar Z, Wheeler MB, Korbutt G, van der Kooy D (2004) Clonal identification of multipotent precursors from adult mouse pancreas that generate neural and pancreatic lineages. Nat Biotechnol 22: 1115-1124

Servitja JM, Ferrer J (2004) Transcriptional networks controlling pancreatic development and beta cell function. Diabetologia 47: 597-613

Song H, Stevens CF, Gage FH (2002) Astroglia induce neurogenesis from adult neural stem cells. Nature 417: 39-44

Stranahan AM, Arumugam TV, Cutler RG, Lee K, Egan JM, Mattson MP (2008) Diabetes impairs hippocampal function through glucocorticoid-mediated effects on new and mature neurons. Nat Neurosci 11: 309-317

Suh H, Consiglio A, Ray J, Sawai T, D'Amour KA, Gage FH (2007) *In vivo* fate analysis reveals the multipotent and self-renewal capacities of Sox2(+) neural stem cells in the adult hippocampus. Cell Stem Cell 1: 515-528

Takizawa T, Nakashima K, Namihira M, Ochiai W, Uemura A, Yanagisawa M, Fujita N, Nakao M, Taga T (2001) DNA methylation is a critical cell-intrinsic determinant of astrocyte differentiation in the fetal brain. Dev Cell 1: 749-758

Tateishi K, He J, Taranova O, Liang G, D'Alessio AC, Zhang Y (2008) Generation of insulin-secreting islet-like clusters from human skin fibroblasts. J Biol Chem 283: 31601-31607

Thorel F, Népote V, Avril I, Kohno K, Desgraz R, Chera S, Herrera PL (2010) Conversion of adult pancreatic α-cells to β-cells after extreme β-cell loss. Nature 464: 1149-1154

Ye P, Carson J, D'Ercole AJ (1995) *In vivo* actions of insulin-like growth factor-I (IGF-I) on brain myelination: studies of IGF-I and IGF binding protein-1 (IGFBP-1) transgenic mice. J Neurosci 15: 7344-7356

Zhang X, Klueber KM, Guo Z, Lu C, Roisen FJ (2004) Adult human olfactory neural progenitors cultured in defined medium. Exp Neurol 186: 112-123

Zhang D, Jiang W, Liu M, Sui X, Yin X, Chen S, Shi Y, Deng H (2009) Highly efficient differentiation of human ES cells and iPS cells into mature pancreatic insulin-producing cells. Cell Res 19: 429-438

Zhao C, Teng EM, Summers RG, Jr, Ming GL, Gage FH (2006) Distinct morphological stages of dentate granule neuron maturation in the adult mouse hippocampus. J Neurosci 26: 3-11

Zhou Q, Brown J, Kanarek A, Rajagopal J, Melton DA (2008) *In vivo* reprogramming of adult pancreatic exocrine cells to beta-cells. Nature 455: 627-632

Zhu W, Shiojima I, Ito Y, Li Z, Ikeda H, Yoshida M, Naito AT, Nishi J, Ueno H, Umezawa A, *et al* (2008) IGFBP-4 is an inhibitor of canonical Wnt signalling required for cardiogenesis. Nature 454: 345-349

World Journal of Neuroscience, 2011, 1, 1-8 WJNS
doi:********** Published Online May 2011 (http://www.SciRP.org/journal/wjns/).

Analyses of fear memory in *Arc/Arg*3.1-deficient mice: intact short-term memory and impaired long-term and remote memory

Kazuyuki Yamada[1*], Chihiro Homma[1], Kentaro Tanemura[3], Toshio Ikeda[2], Shigeyoshi Itohara[2], Yoshiko Nagaoka[1]

[1]Support Unit for Animal Resources Development, Research Resources Center, Brain Science Institute, RIKEN, 2-1 Hirosawa, Wako, Saitama, Japan;
[2]Laboratory for Behavioral Genetics, Brain Science Institute, RIKEN, Hirosawa, Wako, Saitama, Japan;
[3]Division of Cellular & Molecular Toxicology, Biological Safety Research Center, National Institute of Health Sciences, Kamiyoga, Setagaya, Tokyo, Japan.
Email: kaz-yamada@brain.riken.jp

Received ********** 2011.

ABSTRACT

Activity-regulated cytoskeleton-associated protein (Arc/Arg3.1) was originally identified in patients with seizures. It is densely distributed in the hippocampus and amygdala in particular. Because the expression of *Arc/Arg*3.1 is regulated by nerve inputs, it is thought to be an immediate early gene. As shown both *in vitro* and *in vivo*, *Arc/Arg*3.1 is involved in synaptic consolidation and regulates some forms of learning and memory in rats and mice [1,2]. Furthermore, a recent study suggests that Arc/Arg3.1 may play a significant role in signal transmission via AMPA-type glutamate receptors [3-5]. Therefore, we conducted a detailed analysis of fear memory in *Arc/Arg*3.1-deficient mice. As previously reported, the knockout animals exhibited impaired fear memory in both contextual and cued test situations. Although *Arc/Arg*3.1-deficient mice showed almost the same performance as wild-type littermates 4 hr after a conditioning trial, their performance was impaired in the retention test after 24 hr or longer, either with or without reconsolidation. Immunohistochemical analyses showed an abnormal density of GluR1 in the hippocampus of *Arc/Arg*3.1-deficient mice; however, an application of AMPA potentiator did not improve memory performance in the mutant mice. Memory impairment in *Arc/Arg*3.1-deficient mice is so robust that the mice provide a useful tool for developing treatments for memory impairment.

Keywords: Activity-Regulated Cytoskeleton-Associated Protein (Arc/Arg3.1); Knockout (Ko) Mouse; Short-Term Memory; Long-Term Memory; Reconsolidation; Ampa Receptor

1. INTRODUCTION

Activity-regulated cytoskeleton-associated protein (*Arc/Arg*3.1) is encoded by an effector immediate early gene and is selectively localized in neuronal dendrites [6]. *Arc/Arg*3.1 and its encoded protein are thought to play a role in activity-dependent plasticity of dendrites [7]. *Arc/Arg*3.1 mRNA is greatly increased by long-term potentiation (LTP)-inducing electrical stimuli [8,9]; administration of psycho-stimulant drugs such as cocaine [10], amphetamines/methamphetamines [11-13], and phencyclidine [14]; insulin [15], middle cerebral artery occlusion [16], electroconvulsive shock [17,18], olfactory inputs [19], mating [20], stress [21], and other stimuli that prompt neuronal activity [22,23]. The mRNA is then rapidly delivered to the dendrites [9]. Furthermore, intense synaptic activity induces selective localization of *Arc/Arg*3.1 mRNA to activated synapses [9,24]. Therefore, Arc/Arg3.1 is believed to be related to synaptic plasticity, and thus many electrophysiological and biochemical studies have been conducted to investigate this possibility [7-9,25]. These studies have revealed that Arc/Arg3.1 may be a key molecule involved in late-phase LTP, during which long-term memories (LTM) are thought to be established.

Guzowski *et al.* [1] found that rats in which *Arc/Arg*3.1 antisense oligonucleotides were infused into the hippocampus perform relatively poorly in a water-maze probe test. This result strongly suggested that Arc/Arg3.1 plays an important role in the formation of some forms of spatial LTM. Furthermore, Plath et al. [2]

developed *Arc/Arg*3.1-deficient mice and demonstrated learning and memory impairment in these mice in the Morris water maze task, contextual and cued fear conditioning, novel object recognition, and the conditioned taste-aversion test. These results indicate that *Arc/Arg*3.1 regulates a wide range of learning and memory function. According to both behavioral and electrophysiological data, they concluded that *Arc/Arg*3.1 is essential for LTM. Although the authors concluded that Arc/Arg3.1 does not play a significant role in synaptic potentiation and early LTP, they did not show adequate behavioral evidence to conclude the role of *Arc/Arg*3.1 in the fear memory (they only showed intact short-term memory (STM) 10 min after the initial trial, and intact novel object recognition test). LTM deficiency in *Arc/Arg*3.1-deficient mice was evident about 120 min after high-frequency stimuli. Thus, the additional memory tests are necessary that should be conducted at about 120 min or later after the training and/or conditioning.

Arc/Arg3.1 may be involved in the endocytosis of AMPA-type glutamate receptors [3-5] by inducing the internalization of AMPA receptors. The morphological properties of AMPA receptors in *Arc/Arg*3.1-deficient mice were not, however, analyzed, and how AMPA receptor trafficking relates to impaired LTM remains unknown.

Ube3A regulates *Arc/Arg*3.1 degradation in synapses, and mutation of Ube3A may be a cause of autism spectrum disorders [26-28] and Angelman syndrome [29,30]. Using *Ube3A*-deficient mice, Greer et al. [31] recently reported that an increase in *Arc/Arg*3.1 expression leads to a decrease in the number of AMPA receptors. These results suggest that there may be abnormal expression of AMPA receptors in *Arc/Arg*3.1-deficient mice.

In order to elucidate the memory process of *Arc/Arg*3.1-deficient mice, in our current study, we used classical fear conditioning paradigm. First, we confirmed the LTM impairment in *Arc/Arg*3.1-deficient mice. Then, we conducted a time course analysis of the memory impairment of *Arc/Arg*3.1-deficient mice, and assessed the remote memory function of the mutant mice. Furthermore, we compared the brain structure between wild-type and *Arc/Arg*3.1-deficient mice by immunohistochemically.

2. RESULTS

2.1. Successful Generation of *Arc/Arg*3.1-Deficient Mice

We generated *Arc/Arg*3.1-deficient mice with MS12 ES cells derived from the C57BL/6 mouse strain (Supplemental information). Before conducting fear-conditioning experiments, we confirmed the intact pain sensation of *Arc/Arg*3.1-deficient mice with a tail-flick and a hot-plate paradigm in another batch of mice ($n = 10$ each). In both tests, they displayed responses indistinguishable from those of wild-type littermates (data not shown). These results indicated that *Arc/Arg*3.1-deficient mice had normal pain sensation and that they and their wild-type littermates would respond equivalently to electric foot shocks. Therefore, a classical fear-conditioning paradigm was appropriate to assess their memory function.

2.2. *Arc/Arg*3.1-Deficient Mice Exhibited Impairment in Both Contextual Fear and Cued fear Memory

Classical fear conditioning consists of a conditioning phase, a context test, and an auditory cued test. *Arc/Arg*3.1-deficient mice exhibited a clearly lower occurrence of freezing than did wild-type mice in the context test. The mean percentage of freezing frequency was significantly lower in *Arc/Arg*3.1-deficient mice (Mann-Whitney's U-test, U = 15, $p < 0.01$; **Figure 1A**). The subsequent auditory cue test consisted of two parts: the first half was done without a cue to assess the non-specific and/or generalized fear response to the new context, and the latter half was done with an auditory cue to assess the fear response to the cue (**Figure 1B**). The mean freezing frequency of *Arc/Arg*3.1-deficient mice was also significantly lower than that of wild-type mice under both conditions (without cue: Mann-Whitney's U-test, U = 18, $p < 0.05$; with cue: U = 0, $p < 0.001$). The identical tests were replicated five times with both male and female mice. There were no differences in impaired memory performance according to sex. Female *Arc/Arg*3.1-deficient mice did, however, display a significantly lower freezing frequency (data not

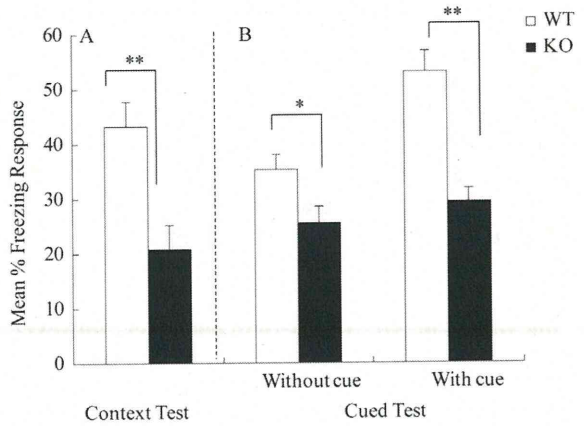

Figure 1. Summary of contextual and cued-fear memory performance of wild-type (WT) and *Arc/Arg*3.1-deficient (KO) mice. (A) Results of the context test. (B) Results of the cued test. Data represent the mean ± S.E.M. Asterisks indicate statistical significance (**, $p < 0.01$; *, $p < 0.05$).

shown). *Arc*/*Arg*3.1-deficient mice showed a significant decrease in the freezing response to the new context without an auditory cue. Because the results of the cued test reflect both generalized contextual fear [32] and cued fear, cued tests may be redundant. Therefore, only the contextual test trial was used in the following experiments.

2.3. *Arc*/*Arg*3.1-Deficient Mice Exhibited Intact STM but Impaired LTM

We conducted fear-conditioning tests to compare STM, LTM, and the retention of LTM in wild-type and *Arc*/*Arg*3.1-deficient mice. In the initial context test (4 hr after conditioning), the mean percentage of freezing of *Arc*/*Arg*3.1-deficient mice was indistinguishable from that of wild-type mice (Mann-Whitney's U-test, $U = 42$, n.s.; **Figure 2**). In the second context test conducted 24 hr after conditioning, the mean percentage of freezing of *Arc*/*Arg*3.1-deficient mice was, however, significantly lower than that of wild-type mice (Mann-Whitney's U-test, $U = 24$, $p < 0.05$; **Figure 2**). In the 1-week and 4-week tests, the mean percentage of freezing of *Arc*/*Arg*3.1-deficient mice was also significantly lower than that of wild-type mice (1-week test: Mann-Whitney's U-test, $U = 2$, $p < 0.01$; 4-week test: Mann-Whitney's U-test, $U = 0$, $p < 0.01$; **Figure 2**). The freezing frequency of wild-type mice increased significantly during the experiment, contrary to that of *Arc*/*Arg*3.1-deficient mice, whose freezing frequency decreased significantly (Two-way ANOVA with repeated measures: genotype, $F(79,1) = 58.5$, $p < 0.001$; retention time, $F(79,3) = 2.47$, $p = 0.07$, n.s.; genotype × retention time, $F(79,3) = 12.6$, $p < 0.001$; wild-type 4 hr vs. 4 week, $t = 3.33$, $p < 0.01$; *Arc*/*Arg*3.1-deficient mice 4 hr vs. 4 week, $t = 4.91$, $p < 0.01$).

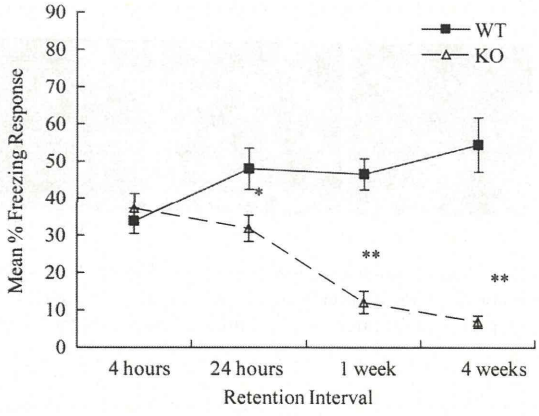

Figure 2. Summary of the STM and LTM tests of wild-type (WT) and Arc/Arg3.1-deficient (KO) mice. Data represent the mean ± S.E.M. Asterisks indicate statistical significance (**, $p < 0.01$; *, $p < 0.05$).

2.4. *Arc*/*Arg*3.1-Deficient Mice Showed Almost No Remote Memory of Fear

As in the STM and LTM test, the same mice were used for all experiments, because the retention curve could have been affected by the repeated exposure to the conditioning context (e.g., reconsolidation, Suzuki et al., [33]). Therefore, we conducted a remote memory test. Mice were conditioned and kept without any treatment except standard daily care for 4 weeks, and then we conducted a context test. Wild-type mice showed a high freezing frequency, but *Arc*/*Arg*3.1-deficient mice did not show any freezing response (Mann-Whitney's U-test: $U = 0$, $p < 0.01$; **Figure 3**).

2.5. AMPA Receptors Were Expressed at Higher Levels in the Hippocampus of Arc/Arg3.1-Deficient Mice

Immunohistochemical analyses were conducted to clarify the distribution of neuronal processes and synapses. Although increased immunoreactivity for neuronal processes (NF-M, MAP1A) was detected in the cerebral cortex of *Arc*/*Arg*3.1-deficient mice, no substantial differences were detected in the hippocampal region (**Figure 4**). Nevertheless, immunoreactivity for pre- and post-synaptic proteins (SYP, HOM) was somewhat increased in the hippocampus of *Arc*/*Arg*3.1-deficient mice (**Figure 4**). We also found increased immunoreactivity for GluR1 in the CA1 region and dentate gyrus (DG) of the hippocampus and for SYP in the CA3 region of *Arc*/*Arg*3.1- deficient mice as compared with that of wild-type mice (**Figure 5**). In order to confirm the increased GluR1 reactivity in hippocampus, we calculated

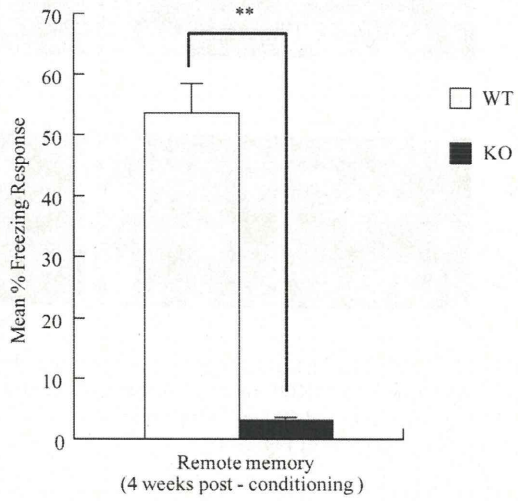

Figure 3. Summary of remote memory test of wild-type (WT) and *Arc*/*Arg*3.1-deficient (KO) mice. Data represent the mean ± S.E.M. Asterisks indicate statistical significance (**, $p < 0.01$).

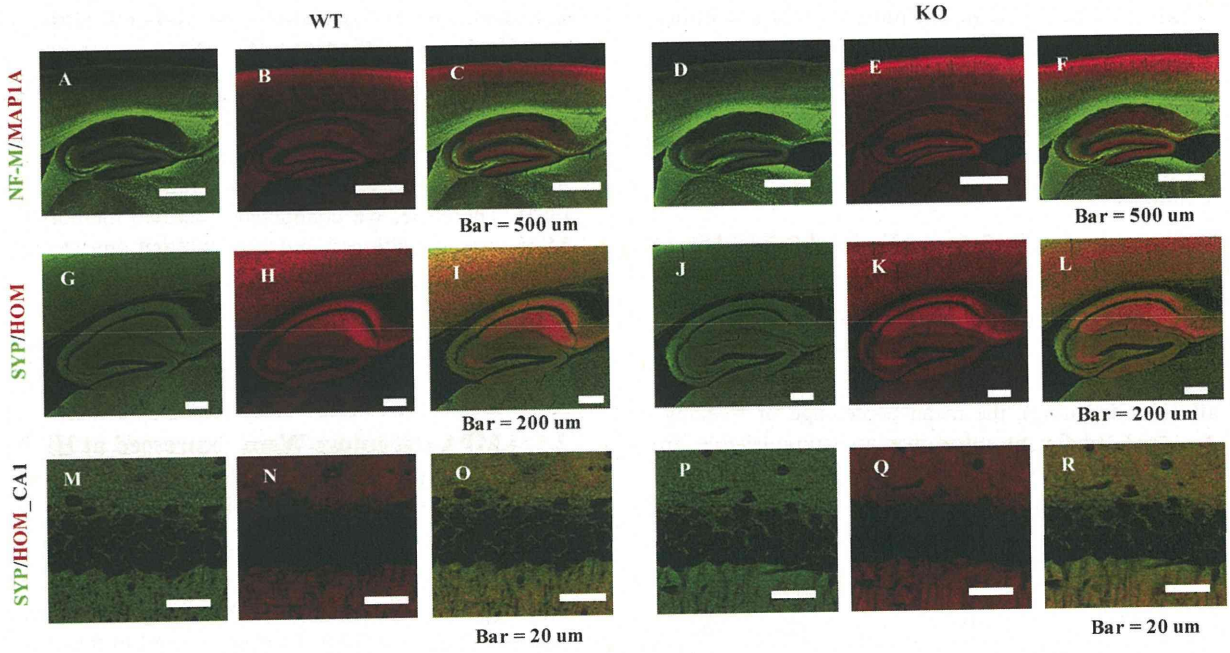

Figure 4. Immunohistochemical analysis of hippocampal neurons and synapses of wild-type (WT) and *Arc/Arg*3.1-deficient (KO) mice. A–F, Immunohistochemical images of neurofilament-m (NF-M; green) and MAP1A (red). G–R, Immunohistochemical images of synaptophysin (SYP; green) and homer (HOM; red). A–C, G–I, and M–O, wild-type mice. D–F, J–L, and P–R, *Arc/Arg*3.1-deficient (KO) mice. C, F, I, L, O, and R, merged images. A–F, cerebral cortex and hippocampus; scale bar = 500 μm. G–L, hippocampus; scale bar = 200 μm. M–R, CA1 region of the hippocampus; scale bar = 20 μm.

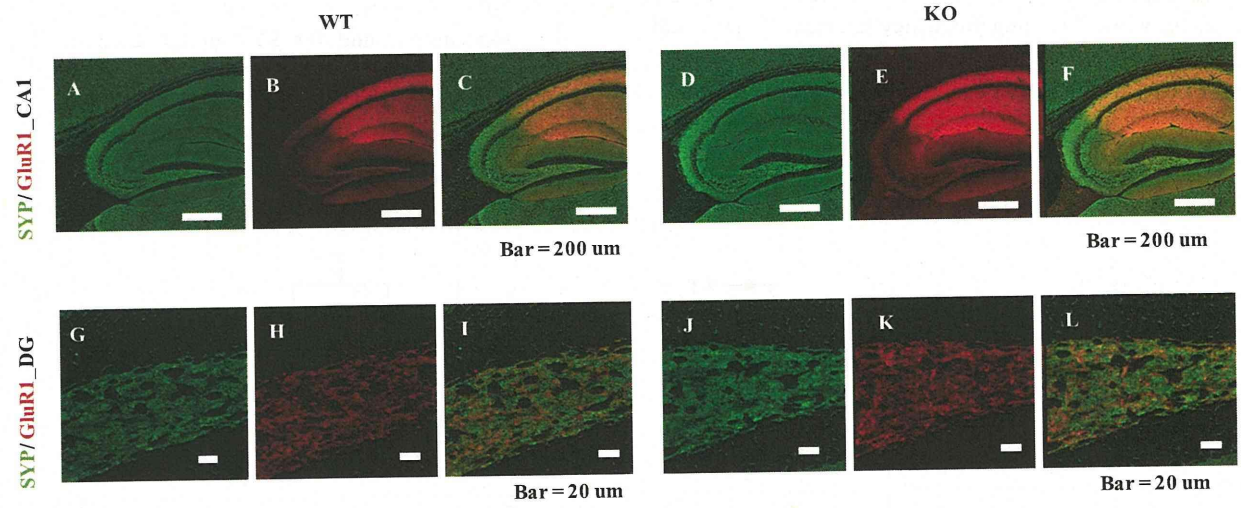

Figure 5. Immunohistochemical analysis of the distribution of AMPA-type glutamate receptors (GluR1) in wild-type and *Arc/Arg*3.1-deficient (KO) mice. Immunohistochemical images of synaptophysin (SYP, green) and AMPA-type glutamate receptors (GluR1, red). A–C and G–I, wild-type mice. D–F and J–L, Arc/Arg3.1-deficient (KO) mice. C, F, I, and L, merged images. Scale bars are identical as those of Figure 4.

the ratio of fluorescence intensity and compared between wild-type and *Arc/Arg*3.1-deficient mice in a semi-quantitative manner. *Arc/Arg*3.1-deficient mice exhibited statistically significant increase of GluR1 immunoreactivity in CA1 and CA3 (both $p<0.01$, **Figure 6**).

3. DISCUSSION

In our current study, we demonstrated impaired fear

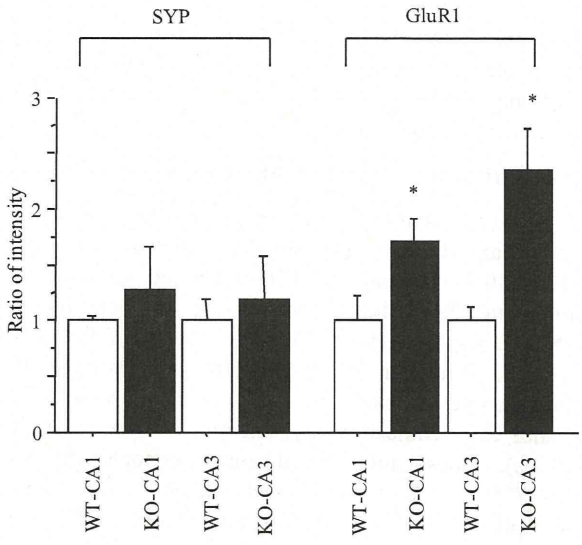

Figure 6. Ratio of fluorescence intensity. SYP: synaptophysin, GluR1: AMPA-type glutamate receptors, WT: wild-type mice, KO: *Arc/Arg3.1*-deficient mice. Data represent mean + SEM. *: $p<0.01$ (compared to wild-type mice).

memory in *Arc/Arg*3.1-deficient mice. In addition, immunohistochemical analysis revealed changes in synaptic structure and increased AMPA receptor expression in the hippocampus of *Arc/Arg*3.1-deficient mice. These findings suggest that *Arc/Arg*3.1 plays crucial roles not only in LTM formation but also in the memory retention process. Although an AMPA potentiator did not lead to recovery of the impaired memory in *Arc/Arg*3.1-deficient mice (Supplemental information and Supplemental **Figure 2**), this is the first study that used *Arc/Arg*3.1-deficient mice to assess the effect of drugs on memory impairment.

*Arc/Arg*3.1-deficient mice exhibited a lower percentage of freezing than did wild-type mice in the context and cued-memory test, indicating that *Arc/Arg*3.1-deficient mice were impaired in both contextual and cued memory. Many studies have reported that contextual fear reflects hippocampus-dependent memory function, and cued fear reflects amygdala-dependent memory function (for review, see LeDoux, [34]). Therefore, *Arc/Arg*3.1-deficient mice may be impaired in both hippocampus- and amygdala-dependent memory function. These results suggest that *Arc/Arg*3.1 may function in the amygdala for auditory fear memory formation as well as in the hippocampus for spatial memory formation. *Arc/Arg*3.1-deficient mice did, however, show a significant decrease in the freezing response to the new context without an auditory cue in the cued test. This result indicates that the freezing response in the cued test may reflect both generalized contextual fear and cued fear. Therefore, new experimental tasks or protocols should be developed to clarify the role of *Arc/Arg*3.1 in amygdala-dependent memory processes.

In this study, we examined STM and LTM in *Arc/Arg*3.1-deficient mice. *Arc/Arg*3.1-deficient mice exhibited unimpaired memory performance 4 hr after conditioning, indicating that their STM or early stage of LTM was intact. In contrast, 24 hr after the conditioning trial, the memory performance of *Arc/Arg*3.1-deficient mice was greatly impaired. After 4 weeks, their memory was almost completely absent, whereas that of wild-type mice slightly but significantly increased. This differential retention process may be partly due to repeated exposure to the conditioning context. Short exposure to conditioned stimuli may enhance fear memory (reconsolidation: [33,35]). Decreased fear memory by repeated exposure indicates that the reconsolidation process may also be impaired in *Arc/Arg*3.1-deficient mice. Thus, we assessed remote memory (ability to retrieve distant episodes/events) directly and confirmed complete impairment of remote memory in *Arc/Arg*3.1-deficient mice.

Immunohistochemical analyses revealed increased expression of AMPA-type glutamate receptors in hippocampal regions. This result is consistent with previous studies reporting that *Arc/Arg*3.1 may be involved in endocytosis of AMPA-type glutamate receptors and may prompt the internalization of AMPA receptors [3-5]. Although LTP, especially early-phase LTP, depends on NMDA receptors ([36] for review), activation of AMPA receptors may improve memory function in rats and mice [37,38]. Therefore, this mutant mouse strain will be useful for developing treatments including drugs for memory impairment.

4. EXPERIMENTAL PROCEDURES

4.1. The Behavioral Laboratory Environment and Housing Conditions of Mice

Mice were housed individually before transfer to the behavioral laboratory. They were kept in the laboratory during the behavioral analysis under a light/dark cycle of 12 hr/12 hr (lights on at 8:00). The laboratory was air conditioned, and the temperature and humidity were maintained at ~22 C – 23°C and 50% – 55%, respectively. Food and water were freely available except during experimentation unless otherwise indicated. We used large tweezers with soft vinyl tips to handle the mice to avoid potential differences in the handling technique of the different researchers involved in the study.

Animal experiments in this study were conducted in strict accordance with the guidelines of the Institute of Physical and Chemical Research (RIKEN) and were approved by the Animal Investigation Committee of the Institute.

4.2. Classical Fear Conditioning

4.2.1 Contextual and Cued Test

Twenty mice (wild type, n = 10; *Arc*/*Arg*3.1 deficient, n = 10; 9 weeks of age) were used. This test consisted of three parts: a conditioning trial, a context test trial, and a cued test trial. Fear conditioning was carried out on a clear plastic chamber equipped with a stainless-steel grid floor (34 × 26 × 30 [H] cm). The luminance of the floor was 225 Lux in the conditioning and context test trial and 0–1 Lux in the cued test trial. A CCD camera was installed on the ceiling of the chamber and was connected to a video monitor and a Windows PC. The grid floor was wired to a shock generator. White noise (65 dB) was supplied from a loudspeaker as an auditory cue (conditioned stimulus, CS). The conditioning trial consisted of a 2-min exploration period followed by two CS–unconditioned stimulus (US) pairings separated by 1 min each. A US (foot-shock: 0.5 mA, 2 sec) was administered at the end of the 30-sec CS period. A context test was performed in the same conditioning chamber for 3 min in the absence of the white noise 24 hr after the conditioning trial. In addition, a cued test was performed in an alternative context with distinct cues: the test chamber was different from the conditioning chamber in brightness (dark environment, almost 0–1 Lux), color (white), floor structure (no grid), and shape (triangular). The cued test was conducted 24 hr after the contextual test was finished, and consisted of a 2-min exploration period (no CS) to evaluate the nonspecific contextual fear followed by a 2-min CS period (no foot shock) to evaluate the acquired cued fear.

4.2.2. STM and LTM test

A second set of mice (wild type, n = 10; *Arc*/*Arg*3.1 deficient, n = 10; 9 weeks of age) was used for these tests. The conditioning trial was the same as in the above contextual and cued test (see 4.2.1). After 4 hr, an STM test was conducted, and LTM tests were conducted 24 hr, 1 week, and 4 weeks later. STM and LTM tests were the same as the context test of 4.2.1. In this test, the cued test was not conducted to exclude any sensitization effect caused by the auditory cue.

4.2.3. Remote memory test

A third set of mice (wild type, n = 10; *Arc*/*Arg*3.1 deficient, n = 10; 9 weeks of age) was used. The conditioning trial was the same as in the above STM and LTM test (see 4.2.2). In this test, a context test was conducted 4 weeks after the conditioning trial.

Both the contextual and cued tests and the STM and LTM tests were replicated five times to confirm their reproducibility. The rate of the freezing response (immobility excluding respiration and heartbeat) of mice was measured as an index of fear memory. Data were collected and analyzed with Image J FZ2 (O'Hara, Tokyo, Japan; Image J XX is modified software based on the public domain Image J program developed at the U.S. National Institutes of Health and is available at http://rsb.info.nih.gov/ij).

4.3. Immunohistochemical Analysis

Brains (n = 4 male mice per group) were fixed with methacarn fixative (methanol/chloroform/acetic acid, 60:30:10 [v/v]), and paraffin-embedded sections were prepared [39]. Mouse monoclonal anti-neurofilament (NF-M, sc-20013; Santa Cruz Biotechnology, CA, USA; 1:1000; a marker for axons), rabbit polyclonal anti-microtubule-associated protein 1A (MAP1A, sc-25728; Santa Cruz Biotechnology; 1:1000; a marker for dendrites), mouse monoclonal anti-synaptophysin (SYP, sc-17750; Santa Cruz Biotechnology; 1:1000; a presynaptic marker), rabbit polyclonal anti-homer (HOM, sc-15321; Santa Cruz Biotechnology; 1:500; a postsynaptic marker), and anti-GluR1(GluR1, sc-28779; Santa Cruz Biotechnology; 1:500) were used for immunohistochemistry. Sections were pretreated with HistoVT-One (Nacalai Tesque, Japan) and incubated with primary antibodies. Signals were visualized with Alexa 568-conjugated anti-mouse IgG and Alexa 488-conjugated anti-rabbit IgG (Molecular Probes, OR). Images were obtained with an FV-300 confocal laser-scanning microscope (Olympus, Japan).

For semi-quantitative analysis of image, the ratio of fluorescence intensity was calculated and compared *Arc*/*Arg*3.1-deficient mice to wild-type by using IMAGE J program (http://rsb.info.nih.gov/ij/index.html. National Institute of Health, Bethesda), after adjusting background noise (n = 4 images per mouse).

5. ACKNOWLEDGEMENTS

We thank Dr. Yoshitake Sano for his comments and suggestions regarding this study. We also thank Dr. Mariko Katayama for her assistance in maintaining the *Arc*/*Arg*3.1-deficient mouse line.

REFERENCES

[1] Guzowski, J., Lyford, G., Stevenson, G., *et al.* (2000) Inhibition of activity-dependent Arc protein expression in the rat hippocampus impairs the maintenance of long-term potentiation and the consolidation of long-term memory. *The Journal of Neuroscience*, **20**, 3993-4001.

[2] Plath, N., Ohana, O., Dammermann, B., *et al.* (2006) *Arc*/*Arg*3.1 is essential for the consolidation of synaptic plasticity and memories. *Neuron*, **52**, 437-444.

[3] Chowdhury, S., Shepherd, J.D., Okuno, H., *et al.* (2006) *Arc*/*Arg*3.1 interacts with the endocytic machinery to regulate AMPA receptor trafficking. *Neuron*, **52**, 445-459.

[4] Rial Verde, E.M., Lee-Osbourne, J., Worley, P.F., *et al.*

(2006) Increased expression of the immediate-early gene arc/arg3.1 reduces AMPA receptor-mediated synaptic transmission. *Neuron*, **52**, 461-74.

[5] Shepherd, J.D., Rumbaugh, G., Wu, J., Chowdhury, S., *et al.* (2006) *Arc/Arg*3.1 mediates homeostatic synaptic scaling of AMPA receptors. *Neuron*, **52**, 475-84.

[6] Steward, O. and Worley, P. (2002) Local synthesis of proteins at synaptic sites on dendrites: role in synaptic plasticity and memory consolidation? *Neurobiology of Learning and Memory*, **78**, 508-527.

[7] Lyford, G., Yamagata, K., Kaufmann, W., *et al.* (1995) Arc, a growth factor and activity-regulated gene, encodes a novel cytoskeleton-associated protein that is enriched in neuronal dendrites. *Neuron*, **14**, 433-445.

[8] Rodríguez, J.J., Davies, H.A., Silva, A.T., *et al.* (2005) Long-term potentiation in the rat dentate gyrus is associated with enhanced *Arc/Arg*3.1 protein expression in spines, dendrites and glia. *European Journal of Neuroscience*, **21**, 2384-2396.

[9] Steward, O, and Worley, P. (2001) A cellular mechanism for targeting newly synthesized mRNAs to synaptic sites on dendrites. *Proceedings of the National Academy of Sciences of the United States of America*, **98**, 7062-7068.

[10] Fosnaugh, J., Bhat, R., Yamagata, K., *et al.* (1995) Activation of arc, a putative "effector" immediate early gene, by cocaine in rat brain. *Journal of Neurochemistry*, **64**, 2377-2380.

[11] Kodama, M., Akiyama, K., Ujike, H., *et al.* (1998) A robust increase in expression of arc gene, an effector immediate early gene, in the rat brain after acute and chronic methamphetamine administration. *Brain Research*, **796**, 273-283.

[12] Moro, H., Sato, H., Ida, I., *et al.* (2007) Effects of SKF-38393, a dopamine D1 receptor agonist on expression of amphetamine-induced behavioral sensitization and expression of immediate early gene arc in prefrontal cortex of rats. *Pharmacology Biochemistry and Behavior*, **87**, 56-64.

[13] Yamagata, K., Suzuki, K., Sugiura, H., *et al.* (2000) Activation of an effector immediate-early gene arc by methamphetamine. *Annals of the New York Academy of Sciences*, **914**, 22-32.

[14] Nakahara, T., Kuroki, T., Hashimoto, K., *et al.* (2000) Effect of atypical antipsychotics on phencyclidine-induced expression of arc in rat brain. *NeuroReport*, **11**, 551-555.

[15] Kremerskothen, J., Wendholt, D., Teber, I., *et al.* (2002) Insulin-inducedexpression of the activity-regulated cytoskeleton-associated gene (ARC) in human neuroblastoma cells requires p21(ras), mitogen-activated protein kinase/extracellular regulated kinase and src tyrosine kinases but is protein kinase C-independent. *Neuroscience Letters*, **22**, 153-156.

[16] Kunizuka, H., Kinouchi, H., Arai, S., *et al.* (1999) Activation of Arc gene, a dendritic immediate early gene, by middle cerebral artery occlusion in rat brain. *NeuroReport*, **10**, 1717-1722.

[17] Larsen, M.H., Olesen, M., Woldbye, D.P., *et al.* (2005) Regulation of activity-regulated cytoskeleton protein (Arc) mRNA after acute and chronic electroconvulsive stimulation in the rat. *Brain Research*, **1064**, 161-165.

[18] Mikkelsen, J. D. and Larsen, M. H. (2006) Effects of stress and adrenalectomy on activity-regulated cytoskeleton protein (Arc) gene expression. *Neuroscience Letters*, **403**, 239-243.

[19] Guthrie, K., Rayhanabad, J., Kuhl, D., *et al.* (2000) Odors regulate Arc expression in neuronal ensembles engaged in odor processing. *NeuroReport*, **11**, 1809-1813.

[20] [20] Matsuoka, M., Yamagata, K., Sugiura, H., *et al.* (2002) Expression and regulation of the immediate-early gene product Arc in the accessory olfactory bulb after mating in male rat. *Neuroscience*, **11**, 251-258.

[21] Montag-Sallaz, M, and Montag, D. (2003) Learning-induced arg 3.1/arc mRNA expression in the mouse brain. *Learning and Memory*, **10**, 99-107.

[22] Kelly, M.P. and Deadwyler, S.A. (2003) Experience-dependent regulation of the immediate-early gene arc differs across brain regions. *The Journal of Neuroscience*, **23**, 6443-6451.

[23] Taishi, P., Sanchez, C., Wang, Y., *et al.* (2001) Conditions that affect sleep alter the expression of molecules associated with synaptic plasticity. *American Journal of Physiology: Regulatory Integrative and Comparative Physiology*, **281**, R839-R845.

[24] Kelly, M.P. and Deadwyler, S.A. (2002) Acquisition of a novel behavior induces higher levels of Arc mRNA than does overtrained performance. *Neuroscience*, **110**, 617-626.

[25] Ons, S., Martí, O. and Armario, A. (2004) Stress-induced activation of the immediate early gene Arc (activity-regulated cytoskeleton-associated protein) is restricted to telencephalic areas in the rat brain: relationship to c-fos mRNA. *Journal of Neurochemistry*, **89**, 1111-1118.

[26] Cook, E.H., Jr., Lindgren, V., Leventhal, B.L., *et al.* (1997) Autism or atypical autism in maternally but not paternally derived proximal 15q duplication. *The American Journal of Human Genetics*, **60**, 928-934.

[27] Glessner, J.T., Wang, K., Cai, G., Korvatsuka, O., *et al.* (2009) Autism genome-wide copy number variation reveals ubiquitin and neuronal genes. *Nature*, **459**, 569-573.

[28] Suteliffe, J.S., Nurmi, E.L. and Lombroso, P.J. (2003) Genetics of childhood disorders: XLVII. Autism, part 6: duplication and inherited susceptibility of chromosome 15q11-q13 genes in autism. *Journal of the American Academy of Child and Adolescent Psychiatry*, **42**, 253-256.

[29] Kishino, T., Lalande, M. and Wagstaff, J. (1997) UBE3A/E6-AP mutations cause Angeleman syndrome. *Nature Genetics*, **15**, 70-73.

[30] Matsuura, T., Sutcliffe, J. S., Fang, P., *et al.* (1997) De novo truncating mutations in E6-AP ubiquitin-protein ligase gene (UBE3A) in Angelman syndrome. *Nature Genetics*, **15**, 74-77.

[31] Greer, P.L., Hanayama, R., Bloodgood, B.L., *et al.* (2010). The Angelman Syndrome protein Ube3A regulates synapse development by ubiquitinating arc. *Cell*, **140**, 704-716.

[32] Radulovic, J., Kammermeir, J. and Spiess, J. (1998) Generalization of fear responses in C57BL/6J mice subjected to one-trial foreground contextual fear conditioning. *Behavioral Brain Research*, **95**, 179-189.

[33] Suzuki, A., Josselyn, S.A., Frankland, P.W., *et al.* (2004) Memory Reconsolidation and Extinction Have Distinct Temporal and Biochemical Signatures. *The Journal of Neuroscience*, **24**, 4787-4795.

[34] LeDoux, J. (1993) Emotional memory: in search of systems and synapses. *Annals of the New York Academy of Sciences*, **702**, 149-157.

[35] von Hertzen, L.S.J. and Giese, K.P. (2005) Memory Reconsolidation Engages Only a Subset of Immediate-Early Genes Induced during Consolidation. *The Journal of Neuroscience*, **25**, 1935-1942.

[36] MacDonald, J.F., Jackson, M.F. and Beazely, M.A. (2006) Hippocampal long-term synaptic plasticity and signal amplification of NMDA receptors. *Critical Reviews in Neurobiology*, **18**, 71-84.

[37] Sekiguchi, M., Yamada, K., Jin, J., *et al.* (2001) The AMPA receptor allosteric potentiator, PEPA ameliorates post-ischemic memory impairment. *NeuroReport*, **12**, 2947-2950.

[38] Yamada, D., Zushida, K., Wada, K., *et al.* (2009) Pharmacological Discrimination of Extinction and Reconsolidation of Contextual Fear Memory by a Potentiator of AMPA Receptors. *Neuropsychopharmacology*, **34**, 2574-2584

[39] Tanemura, K., Igarashi, K., Matsugami, T-R., *et al.* (2009) Intraurine environment-genome interaction and children's development (2): eBrain structure impairment and behavioral disturbance induced in male mice offspring by a single intraperitoneal administration of domoic acid (DA) to their dams. *The Journal of Toxicological Sciences*, **34**, SP279-286.

Abbreviations

Arc/Arg3.1: activity-regulated cytoskeleton-associated protein; LTP: long-term potentiation; LTM: long-term memory; STM: short-term memory; NF-M; neurofilament-M MAP1A; Microtubule-associated protein 1A; SYP; synaptophysin; HOM; homer; DG: dentate gyrus

SCIENTIFIC REPORTS

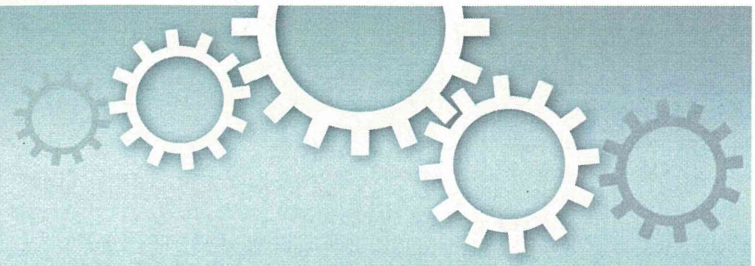

OPEN

SUBJECT AREAS:
BEHAVIOUR
GENETIC POLYMORPHISM
NEUROANATOMY
NEURODEVELOPMENTAL DISORDERS

Received
18 April 2011

Accepted
23 May 2011

Published
17 June 2011

Correspondence and requests for materials should be addressed to J.A. (jaruga@brain.riken.jp)

* These authors contributed equally to this work.

‡ Present address: Division of Molecular Biology, Institute of Medical Science, The University of Tokyo, Minato-ku, Tokyo 108-8639, Japan.

Zic2 hypomorphic mutant mice as a schizophrenia model and *ZIC2* mutations identified in schizophrenia patients

Minoru Hatayama[1]*, Akira Ishiguro[1]*‡, Yoshimi Iwayama[2], Noriko Takashima[1], Kazuto Sakoori[1], Tomoko Toyota[2], Yayoi Nozaki[1], Yuri S. Odaka[1], Kazuyuki Yamada[3], Takeo Yoshikawa[2] & Jun Aruga[1]

[1]Laboratory for Behavioral and Developmental Disorders, [2]Laboratory for Molecular Psychiatry, and [3]Support Unit for Animal Experiments, RIKEN Brain Science Institute, Wako-shi, Saitama 351-0198, Japan.

***ZIC2* is a causal gene for holoprosencephaly and encodes a zinc-finger-type transcriptional regulator. We characterized *Zic2*$^{kd/+}$ mice with a moderate (40%) reduction in *Zic2* expression. *Zic2*$^{kd/+}$ mice showed increased locomotor activity in novel environments, cognitive and sensorimotor gating dysfunctions, and social behavioral abnormalities. *Zic2*$^{kd/+}$ brain involved enlargement of the lateral ventricle, thinning of the cerebral cortex and corpus callosum, and decreased number of cholinergic neurons in the basal forebrain. Because these features are reminiscent of schizophrenia, we examined *ZIC2* variant-carrying allele frequencies in schizophrenia patients and in controls in the Japanese population. Among three novel missense mutations in ZIC2, R409P was only found in schizophrenia patients, and was located in a strongly conserved position of the zinc finger domain. Mouse Zic2 with the corresponding mutation showed lowered transcription-activating capacity and had impaired target DNA-binding and co-factor-binding capacities. These results warrant further study of ZIC2 in the pathogenesis of schizophrenia.**

Zic2/ZIC2 is a member of the Zic family of zinc finger proteins, which function as transcriptional regulators with critical roles in neural development[1–5]. In humans, haploinsufficiency of *ZIC2* results in holoprosencephaly (HPE)[6,7] in which the formation of medial forebrain structures is disturbed. *ZIC2* mutations are found in 3%–4% of unrelated individuals with isolated HPE[7]. Mice homozygous for a hypomorphic mutation in *Zic2* (*Zic2*$^{kd/kd}$) show embryonic or perinatal lethality with HPE-like symptoms and other anomalies[8–11], suggesting that the role of *Zic2* in forebrain development is largely conserved between human and mouse.

The role of Zic2 in embryonic development has been well-studied, but its role in the mature brain and/or the consequences of developmental Zic2 insufficiency in mature animals has not been fully investigated. It is possible that hypomorphic mutations that do not cause embryonic/perinatal lethality have a profound influence on higher brain functions. A pilot investigation analyzing the behavior of mice heterozygous for the hypomorphic mutation in *Zic2* (*Zic2*$^{kd/+}$) showed some abnormalities of the acoustic startle response[12]. However, the behaviors examined in that study were limited. A more comprehensive analysis is needed to clarify the causal relationship between the hypomorphic in *Zic2* and behavioral abnormalities that might underlie neuropsychiatric disorders such as schizophrenia.

Schizophrenia is a relatively common mental disorder that affects 1% of the population worldwide. The disease is characterized by positive symptoms (delusions and hallucinations), negative symptoms (affective flattening and social withdrawal), and cognitive dysfunction (deficits in working memory, attention, processing speed, and executive function)[13,14]. Morphologically, there are abnormalities of the brain that are frequently found in schizophrenia, such as enlarged ventricles, dendritic changes in the pyramidal neurons, and alteration of specific subtypes of interneurons[15–18]. Although the molecular basis of the disease is not fully understood, rare gene mutations that exert large effects in the susceptibility of schizophrenia, in addition to multiple common single nucleotide polymorphisms (SNPs), are being accumulated[19–22].

Here, we first performed comprehensive analyses of the *Zic2*$^{kd/+}$ mice in manifold behavioral test situations and by morphological and histological examinations. Then, since the results suggested that the *Zic2*$^{kd/+}$ mice mimic the schizophrenia-like phenotypes, we undertook resequencing analysis of the *ZIC2* gene using DNA isolated from patients with schizophrenia and from controls. One mutation, R409P, was shown to have impaired transcription activity, DNA-binding ability, and cofactor-binding capacity. These results were discussed in terms of the pathogenesis of schizophrenia.

Results

Wild-type ($Zic2^{+/+}$) and $Zic2^{kd/+}$ mice are indistinguishable by their body weight and external appearance[12]. Both male and female $Zic2^{kd/+}$ mice are fertile and female $Zic2^{kd/+}$ mice can foster their progenies without any obvious faults[8]. In our previous study, we found that prepulse inhibition (PPI) of acoustic startle response is decreased in $Zic2^{kd/+}$ mice[12]. For a more comprehensive analysis of behavioral phenotypes, we carried out the suite of behavioral tests listed in Table 1. For the light-dark box test, marble burying test, elevated plus maze test, forced swimming test, grip strength test, wire hanging test, footprint test and rotarod test, we found no significant differences in behavior between $Zic2^{kd/+}$ and wild-type mice (Table 1)[12]. For the remaining tests, we found significant differences in behavior between $Zic2^{kd/+}$ and wild-type mice; as described below.

Locomotor activities were lower or higher in $Zic2^{kd/+}$ mice than wild-type mice depending on the situation. We first placed the mice in new home cages and then monitored their locomotor activity continuously for 13 days (Figure 1A–C). Our analysis revealed that the locomotor activity was significantly lower in $Zic2^{kd/+}$ mice than in wild-type mice in the later stationary period (relatively low day-to-day variance, days 6–13) ($P = 0.044$) (Figure 1A). When we assessed the mean circadian locomotor activities during the stationary period, we found that the activity of $Zic2^{kd/+}$ mice was significantly lower than that of the wild type in the early dark phase (20:00–24:00) ($P = 0.048$), but that the circadian rhythm of the $Zic2^{kd/+}$ mice was normal (Figure 1B).

We also assessed locomotor activity in open field tests with observation times of 15 min. $Zic2^{kd/+}$ mice showed a significantly higher overall locomotor activity compared to wild-type mice ($P = 0.041$) (Figure 1C, left), but there were no differences in preference between the two genotypes for the central and peripheral fields (Figure 1C, right). These results suggest that $Zic2^{kd/+}$ mice have higher locomotor activities than the wild type in a novel environment.

Cognitive function deficits in $Zic2^{kd/+}$ mice. The Morris water maze test is commonly used to evaluate learning ability and acquisition of spatial memory. In our study, this test consisted of 4 days of training (day 1–4) with a fixed hidden platform, 1 day (day 5) of a probe test without a platform, and 1 day (day 6) of a reverse test in which the hidden platform was placed in the opposite quadrant. To reach the hidden platform, $Zic2^{kd/+}$ mice needed a significantly longer time in the training session ($P = 0.046$) and a significantly longer time in the reverse test session ($P = 0.037$) (Figure 2A, top panel). The moving speed of $Zic2^{kd/+}$ mice was slightly, and significantly, lower than that of wild-type mice only on day 1 of the training session (Figure 2A, left middle panel, $P = 0.036$). However, their spatial memory acquisition was not impaired as seen in the results of the probe test (Figure 2A, bottom panel). The motor performance and motivation of $Zic2^{kd/+}$ mice might not be impaired, given that there were no significant differences between the two genotypes in the moving speed at days 2 to 4 [$F(1,18) = 0.017$, $P = 0.90$, RMANOVA, main effect of genotype] (Figure 2A, left middle panel) or in the overall no movement time [$F(1,18) = 0.23$, $P = 0.64$, RMANOVA, main effect of genotype] (Figure 2A, right middle panel). Further supporting this notion, the results were similar for $Zic2^{kd/+}$ and wild-type mice for the other tests related to motor performance and motivation (rotarod, footprint, wire hanging and forced swimming test) (Table 1). Therefore, the water maze test results were considered to reflect an impaired learning ability of $Zic2^{kd/+}$ mice.

Fear conditioning is a test for associative learning that depends partly on hippocampal function, as is the Morris water maze test. The association of conditioned stimuli (CS, tone) and unconditioned noxious stimuli (US, electric foot shock) was learned in the conditioning on day 1. The results were quantitatively evaluated by the freezing response of the subjects. $Zic2^{kd/+}$ mice showed a significantly reduced freezing response in the context test on day 2 ($P = 0.037$, U-test, Figure 2B). These mice also showed a significantly reduced freezing response in the cue test on day 3 ($P = 0.049$, U-test, Figure 2C).

We also observed abnormal behavioral traits in $Zic2^{kd/+}$ mice in the Y-maze spontaneous alternation test. $Zic2^{kd/+}$ mice showed a significantly lower alteration percentage ($P = 0.046$, U-test) and a significantly higher number of arm entries ($P = 0.0040$) than the wild-type mice (Figure 2C), suggesting that $Zic2^{kd/+}$ mice have working memory impairment and a higher level of locomotor activity in a novel environment. Together with the absence of behavioral traits related to mood disturbances or anxiety-like behaviors, our results from the water maze, fear-conditioning and Y-maze tests are consistent with the impaired cognitive function in $Zic2^{kd/+}$mice.

Abnormalities in social behavior in $Zic2^{kd/+}$ mice. We next assessed the social behaviors of the $Zic2^{kd/+}$ mice by the resident-intruder assay. Juvenile wild-type mice were placed into the home cages of

Table 1 | Summary of $Zic2^{kd/+}$ behavioral analysis.

Test	Response[1]	Implication to schizophrenia[2]
Home cage activity	decreased*	Negative?
Open field		
Locomotor	increased*	Positive (psychomotor agitation)
% center	no change	
Morris Water Maze		
Latency-training	increased*	Cognitive (learning deficits)
Latency-reverse	increased*	
Probe test	no change	
Speed-training	initially slow*	
No move-training	no change	
Fear conditioning		
Conditioning	no change	Cognitive (fear memory deficits)
Contextual	decreased*	
Cue	slightly decreased*	
Y-maze		
No. of entries	increased*	Positive (psychomotor agitation)
% alteration	decreased*	Cognitive (working memory deficits)
Social interaction		
Novel environment	no change	Negative (social withdrawal)
Resident intruder	attack decreased*	
Social dominance	often loser*	Negative (social withdrawal)
Social recognition	no change	Cognitive (sensorimotor gating)
Acoustic startle response	increased*[3]	
PPI of acoustic startle response	decreased*[3]	Cognitive (sensorimotor gating)
Light-Dark box	no change	
Marble burying	no change	
Burrowing	no change	
Elevated Plus maze	no change[3]	
Forced swimming	no change[3]	
Tail suspension	no change	
Grip strength	no change[3]	
Wire hanging	no change[3]	
Footprint	no change[3]	
Rotarod	no change[3]	

[1] $Zic2^{kd/+}$ compared to $Zic2^{+/+}$; [2]Possible relevance to the three classes of schizophrenia symptoms (positive, negative, and cognitive dysfunction); [3] Ogura et al. (2001) [12]; *$P < 0.05$ in statistical tests between $Zic2^{-/-}$ and $Zic2^{kd/+}$.

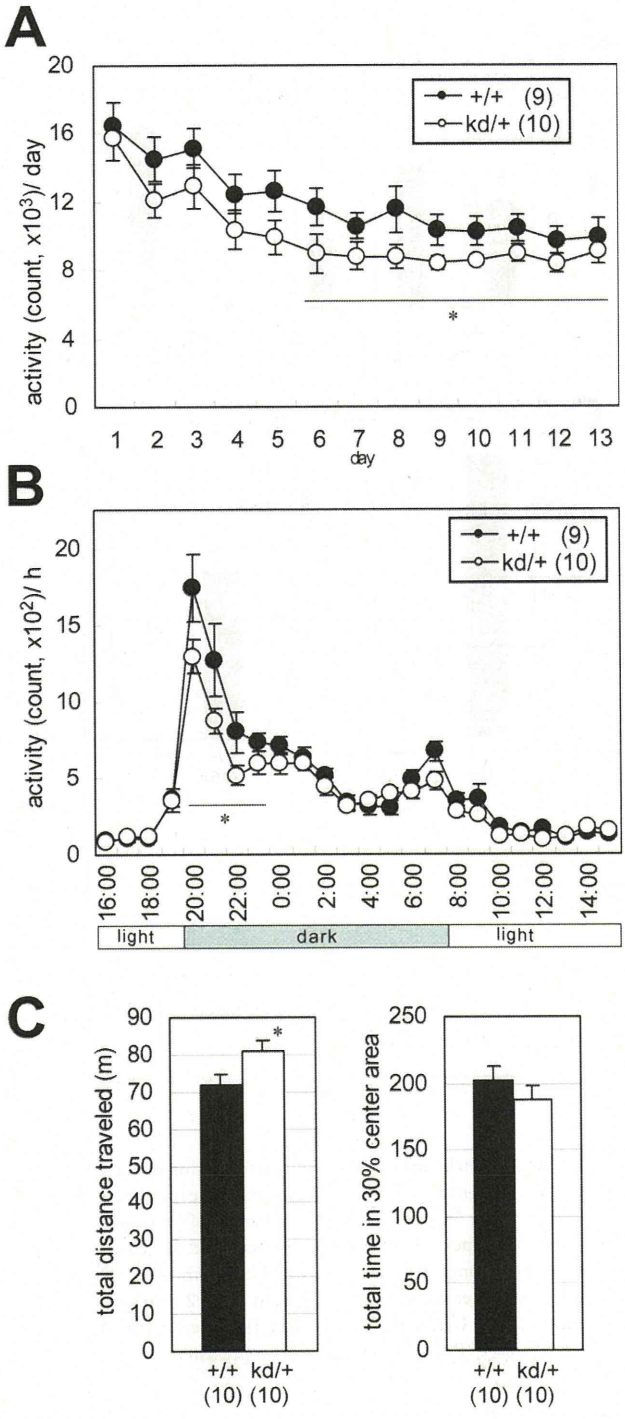

Figure 1 | Spontaneous motor performance abnormalities in *Zic2*$^{kd/+}$ mice. (A) Home cage activity was measured for 13 days. On day 1 the mice were put into a new home cage. Mean activities per day are indicated. Activity counts represent the number of time bins (approximately 0.20–0.25 s each) in which spontaneous activity including locomotor activity, rearing, and other activities such as stereotypic movements, were detected. *$P < 0.05$ in t-test. (B) Circadian activities. The values indicate the summation of the activities corresponding time bins (bin= 1 h) of the last 8 days (days 6–13) when the daily change in the total activity level (A) was minimal. *$P < 0.05$ in t-test. (C) Open field test. (left) Total distance traveled in the open box for 15 min observation period. (right) Percentage of the total time in the central area of the field (30% of the total field area). *$P < 0.05$ in t-test. Data is presented as means ± SEM. The number of mice in each group is given in parentheses.

the resident *Zic2*$^{kd/+}$ mice and the behavior of the test mice (*Zic2*$^{kd/+}$ mice or control wild-type mice) were analyzed for 15 min (Figure 3A, 3B, supplemental video). The time spent attacking ($P = 0.049$; Figure 3A, left panel) and the frequency of attacks were significantly lower in *Zic2*$^{kd/+}$ mice than in control wild-type mice ($P = 0.049$; Figure 3A, right panel). The frequency of body contact also tended to be higher in *Zic2*$^{kd/+}$ mice than in wild-type mice ($P = 0.12$). We also observed abnormal social behavior in *Zic2*$^{kd/+}$ mice in the social dominance tube test (Figure 3C). In this test, *Zic2*$^{kd/+}$ mice and control wild-type mice were placed at opposite ends of a transparent plastic tube in a head-to-head direction, and the first mouse to escape was judged the loser (Figure 3B). In general, mice of both genotypes moved forward and pushed each other within the tube. *Zic2*$^{kd/+}$ mice became losers more frequently than the wild-type mice ($P = 0.024$, chi-square test). We also performed a social interaction test in a novel environment (open field) with caged (Figure S1B) and non-caged partners (Figure S1A), but found no clear differences in the number and duration of the contacts between *Zic2*$^{kd/+}$ and wild-type mice.

Zic2$^{kd/+}$ mouse brain shows an altered morphology and reduction of forebrain cholinergic neurons and amygdalar Zic-positive cells. To elucidate the molecular basis of the behavioral abnormalities observed in *Zic2*$^{kd/+}$ mice, we performed a morphometric analysis of the *Zic2*$^{kd/+}$ mouse brain by MRI (Figure 4). We showed that *Zic2*$^{kd/+}$ mouse brains had enlarged lateral ventricles compared with the brains of wild-type mice (Figure 4A and B). The ratio of the volume of lateral ventricles to brain was 35% higher in the brains of *Zic2*$^{kd/+}$ mice than in those of wild-type mice. The 3D superimposition of lateral ventricles in the brain indicated that the enlargement was most notable in the anterior horn region (Figure 4B and C). Enlargement of the lateral ventricles in *Zic2*$^{kd/+}$ mice might partly reflect the reduction in the mass of the septum (Figure 4A, right panel), which we also observed in MRI 2D coronal images through the anterior commissure (data not shown). The hippocampal size did not show any clear differences between the two genotypes. Morphometric analysis of histological sections revealed that compared to the wild type the thickness of the cerebral cortex and the corpus callosum was slightly but significantly thinner in *Zic2*$^{kd/+}$ mice (cerebral cortex, $P = 0.0038$; corpus callosum, $P = 0.0028$; Figure 4D) and that the position and shape of the medial structure rostral to the hippocampus (fimbria including septofimbrial nucleus or septal triangular nucleus) were significantly narrower ($P < 0.001$ for both, Figure 4D).

We also found the amygdala in *Zic2*$^{kd/+}$ mice to be morphologically different to that in wild-type mice. In wild-type mice, Zic-positive cells were abundant in the amygdalohippocampal area (AHA) and sparse in the medial and cortical nuclei (Figure 4E). In *Zic2*$^{kd/+}$mice, the Zic-positive cells were less abundant than in wild-type mice in the equivalent rostrocaudal positions (Figure 4E, 8/8). Furthermore, the high cell density in the AHA of wild type animals shown in toluidine blue staining seemed reduced and the intense signals detected by acetylcholine esterase staining in the AHA was debilitated (Figure 4E), in *Zic2*$^{kd/+}$ mice. As shown by acetylcholine esterase stained sections (Figure 4E), in some cases (6/8), the medial protrusion of the amygdala in the coronal sections tended to be blunted in *Zic2*$^{kd/+}$ mice compared to the wild type.

The reduction of the septal mass and expression of *Zic2* in the basal forebrain structures[10] led us to investigate the number of cholinergic neurons that are densely distributed in the septum. We counted the choline acetyl transferase (ChAT)-positive cholinergic neurons in comparable coronal sections from the brains of *Zic2*$^{kd/+}$ and wild-type mice. The results indicated that the numbers of cholinergic neurons were decreased in the medial septum, diagonal band and substantia innominata regions, but not in other regions including cerebral cortex, striatum and caudoputamen, (Figure 5A–C). In

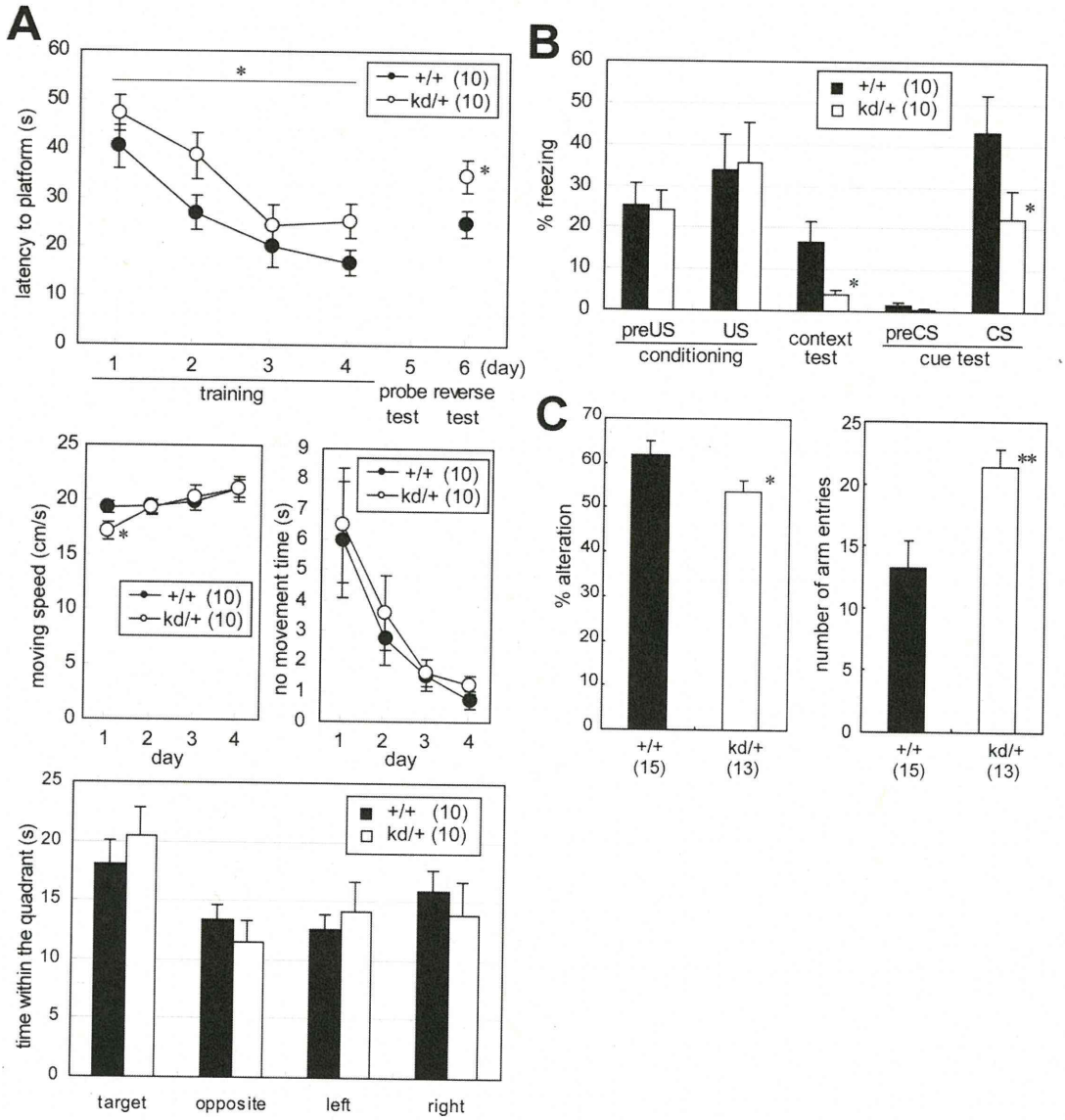

Figure 2 | Cognitive function deficits in *Zic2*$^{kd/+}$ mice. (A) Morris water maze test. (top) Mean latency to reach the platform during the training session (days 1–4) and reverse test session (day 6). Values indicate the mean of all six trials on the day. (middle left) Moving speed in the training session. (middle right) No movement time in the training session. (bottom) The results of the probe test (day 5) as indicated by the period of time (s) in the indicated quadrant within the 60 s testing period. *$P < 0.05$ in t-test. (B) Fear conditioning test. Mean percentage freezing are indicated for the conditioning test (day 1) before and after the electrical foot shock (preUS [mean of the 2 min before unconditioned-stimulus, US] and US [1 min after US] respectively), context test (day 2, mean of the total testing period [5 min]), and cue test (day 3) before and after pre tone (preCS [mean of the 2 min before conditioned stimulus, CS] and CS [mean of the 2 min with CS], respectively). *$P < 0.05$ in Mann-Whitney U-test. (C) Y-maze test. (left) Percentage altered selection of the entered arm. (right) Total number of arm entries. *$P < 0.05$ in Mann-Whitney U-test; **$P < 0.01$ in t-test. Data is presented as means ± SEM. The number of mice in each group is given in parentheses.

addition, the numbers of PV-positive neurons were not different in the medial septum or diagnonal band (Figure 5D). Therefore, the number of basal forebrain cholinergic neurons is selectively reduced by the reduction of *Zic2* expression. We also examined the number of ChAT-positive cells with or without Zic-like immunoreactivities in the affected regions (medial septum, diagonal band and substantia innominata) at early postnatal stages (P5–7, Figure 5E). In *Zic2*$^{kd/+}$ mice, we observed a significant reduction in the number of Zic$^-$ChAT$^+$ cells in the diagonal band region compared to the number in wild-type mice ($P < 0.001$, Figure 5E, left panel). The number of Zic$^-$ChAT$^+$ cells in the medial septum and Zic$^+$ChAT$^+$ cells in the diagonal band and medial septum region also tended to be reduced in *Zic2*$^{kd/+}$ mice compared to the wild type (Zic$^-$ChAT$^+$ cells in the medial septum, $P = 0.062$; Zic$^+$ChAT$^+$ cells in the diagonal band and medial septum region, $P = 0.12$ and $P = 0.056$ respectively). These results were consistent with those obtained in adult mice, suggesting that the reduction in the number of ChAT-positive neurons in the basal forebrain primarily stemmed from the reduction in *Zic2* gene expression during embryonic or prenatal development. In addition, we found that the number of Zic$^+$ChAT$^-$ cells was significantly increased in the diagonal band region and medial septum in *Zic2*$^{kd/+}$ mice compared to wild-type mice (diagonal band, $P = 0.039$; medial septum, $P = 0.047$ respectively; Figure 5E, right panel).

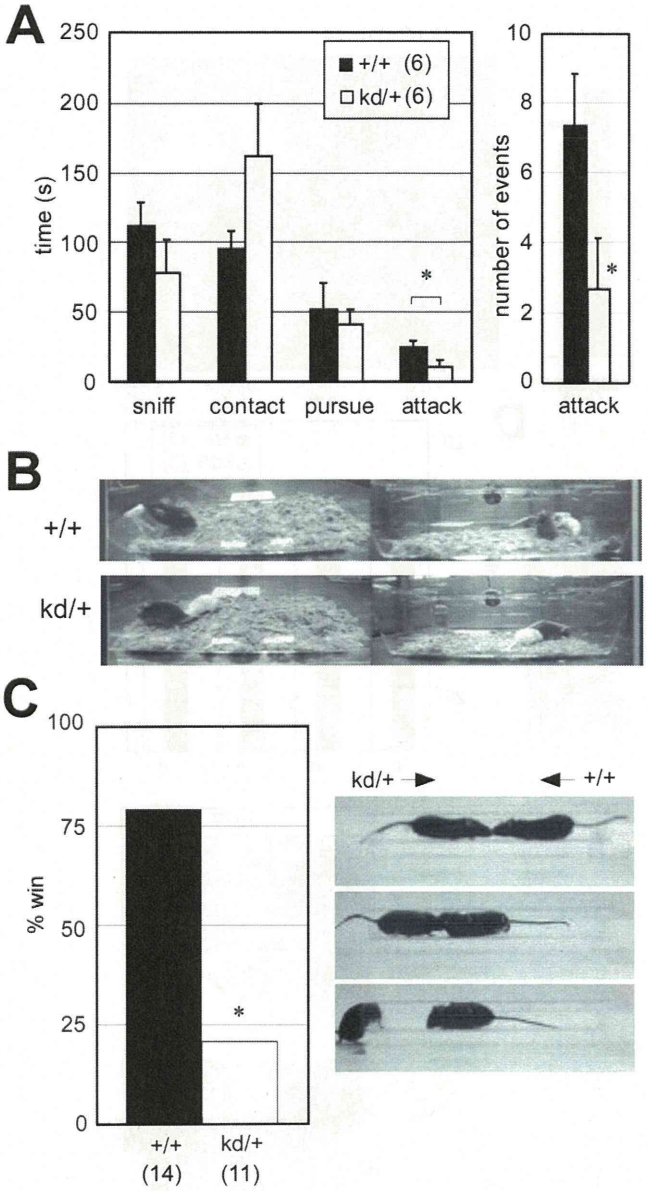

Figure 3 | Social behavior abnormalities in *Zic2*$^{kd/+}$ mice. (A) Resident-intruder test. (left) Total time spent in the indicated behaviors. (right) The number of attacking events. *$P < 0.05$ in t-test. Data is presented as means ± SEM. (B) Captured video image of the resident-intruder test. In this case, the *Zic2*$^{+/+}$ mouse (+/+, top, black) was attacking the white intruder mouse, whereas the *Zic2*$^{kd/+}$ mouse (kd/+, bottom black) was moving away from the intruder mouse. The left and right images indicate the simultaneous recording from opposite directions. (C) Social dominance tube test. (left) Won rate in the total of 66 matches. The means ± SEM latencies to win were as follows: *Zic2*$^{+/+}$, 36.5 ± 5.2; *Zic2*$^{kd/+}$, 38.3 ± 6.4 s. (right) Captured video images from a representative match. From top to bottom, the beginning to the end of the match is sequentially indicated. In this case, the *Zic2*$^{kd/+}$ mouse was pushed out from the plexiglass tube (30 cm) and the *Zic2*$^{+/+}$ mouse became the winner. *$P < 0.05$ in chi-square test. The number of mice in each group is given in parentheses.

Screening of *ZIC2* mutations in patients with schizophrenia. Some of the above behavioral and histological abnormalities in *Zic2*$^{kd/+}$mice are reminiscent of schizophrenia symptoms in humans. We therefore set out to examine whether *ZIC2* mutations contribute to the onset of schizophrenia, in at least a subset of patients. As a first step to address this possibility, we searched *ZIC2* for nonsynonymous mutations in patients with schizophrenia. Many nonsynonymous mutations are reported in patients with HPE[6,23]; however, there are no reports of an association of *ZIC2* mutations with psychiatric illnesses.

Sequence analysis of the entire *ZIC2* protein coding regions and adjacent introns in 278 patients revealed four nonsynonymous mutations in the coding regions (Table 2). We then examined the allele frequencies of these mutations in 967 patients with schizophrenia and in 1060 control subjects (Table 2). Ins239H was the most commonly detected mutation, but its frequency (~9%) was similar in patient and control groups. This finding is consistent with the results of previous studies[7,24–27]. The three remaining mutations, A95T, R409P, and S444R, were novel. A95T and R409P were singleton mutations not found in normal subjects. The frequency of S444R was not significantly different between the patient group (0.39%) and normal subjects (0.18%; $P = 0.80$ by Fisher's exact test). Patients with this mutation showed no obvious psychotic symptoms; however, we could not perform detailed physical examinations on these patients, nor examine the genotypes of their relatives because we could not obtain their consent on these issues.

The *Zic2*-R409P shows impaired transcriptional activation. Zic orthologues are widely distributed among the eumetazoans and show evolutionary conserved domains in their protein-coding regions[28]. Multi-species alignment of the three *Zic2* mutations revealed that R409P was located within the highly conserved regions of the published Zic sequences, including those of the protostomians and cnidarians (Figure 6A and data not shown). We also showed that R409 position has conserved in a zinc-finger-type transcription factor, GLI1, in which the side chain of the encoded amino acid residue is responsible for side-chain-base interactions (Figure S2)[29]. Both A95T and S444R were conserved in most of the vertebrate *Zic2* sequences examined, but these sequences did not align with those in invertebrates (Figure 6A and data not shown). We used the computer algorithm PolyPhen Polyphen[30] to predict the effect of the mutations on protein structure and function. PolyPhen analysis predicted that the amino acid change in R409P most likely caused abnormal protein structure and function, whereas it was only a possibility for S444R and even less likely for A95T (Table 2).

We characterized the function of these mutations by generating the equivalent mutations in mouse Zic2 proteins, and assessing their activities in vitro. The size of the mutant Zic2 proteins was mostly comparable to that of the wild type protein, as shown by sodium dodecyl sulfate-polyacrylamide gel electrophoresis (SDS-PAGE) analysis (Figure 6B). However, the band corresponding to Zic2-S444R also contained a fast migrating component in preparations from both transfected mammalian cells and from in vitro translation (Figure 6B and data not shown). The nuclear localization capacity of the mutant proteins was significantly reduced for R409P ($P < 0.001$ in chi-square test), but not for A95T or S444R (Figure S2). Zic2 can be a transcriptional activator[31,32]. We assessed the transactivating activity of the mutant proteins by co-transfecting mammalian cells with expression vectors that express the proteins. The Zic2-R409P protein, but not the Zic2-A95T or Zic2-S444R proteins had significantly reduced transactivating capacity compared to the wild-type protein ($P < 0.001$, Figure 6C); the normalized activation capacity of Zic2-R409P was approximately 20% that of the wild-type protein. When we examined the effect of the R409P mutation on the capacity to bind a high-affinity Zic-binding sequence, Zic2-R409P showed lower binding affinity to the target sequences than wild-type Zic2 (Figure 6D and 6E). Zic2 is known to complex with the DNA-PK catalytic subunit and RHA[33]. As shown in immunoprecipitation experiments (Figure 6F), the binding affinity of Zic2-R409P to DNA-PK, but not to RHA, was reduced compared to wild-type

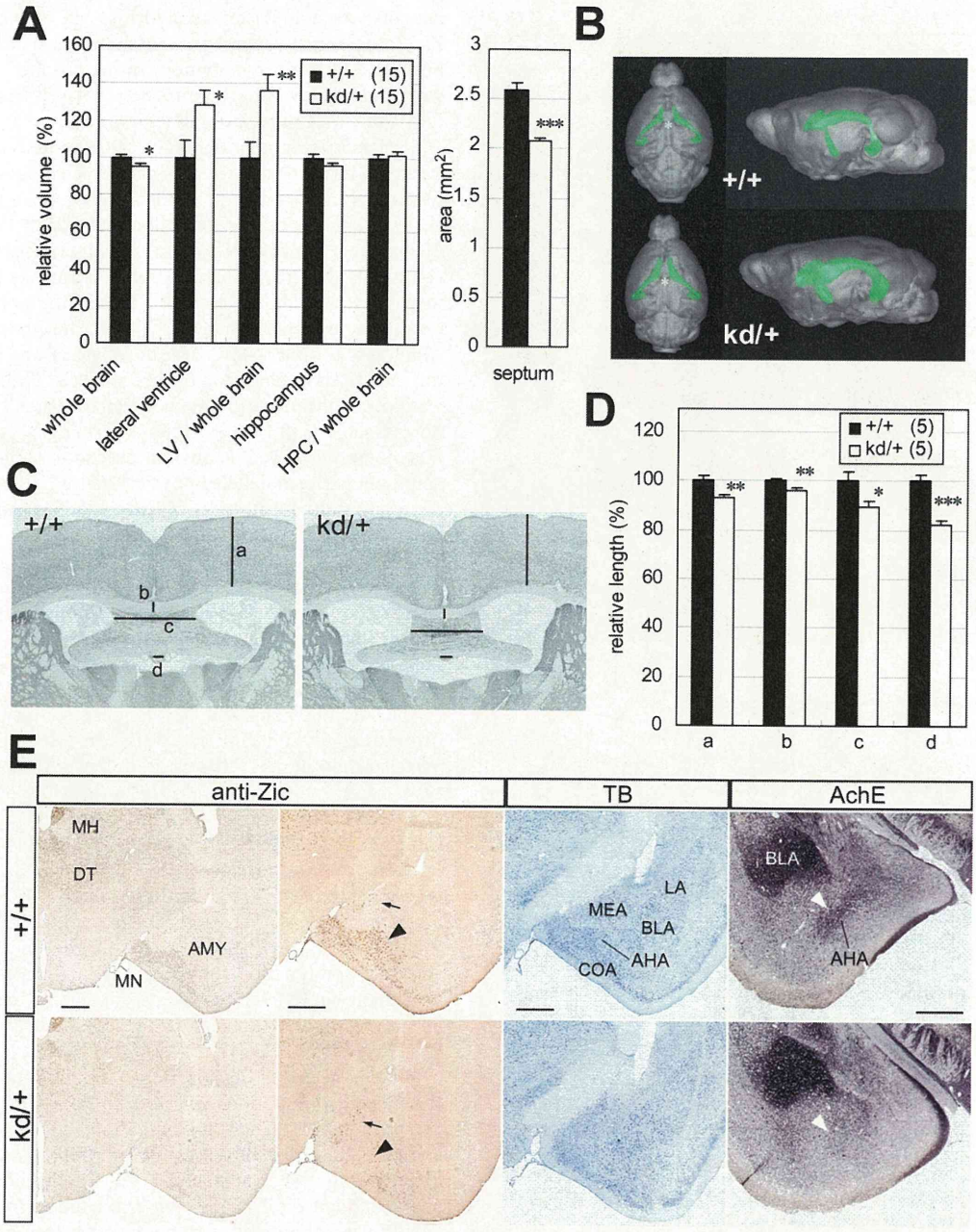

Figure 4 | Morphological features of the brains from *Zic2*$^{kd/+}$ mice. (A) Volumetric analysis of the entire brain, lateral ventricle (LV), and hippocampus (HPC). The values for tissue volumes in *Zic2*$^{kd/+}$ mice are indicated as percentages of the corresponding wild-type values. The values for ratio of volumes in LV/whole brain and HPC/whole brain are also indicated as percentages of the corresponding wild-type values. A total of 15 pairs of *Zic2*$^{+/+}$ and *Zic2*$^{kd/+}$ mice were subjected to in vivo MRI imaging. *$P < 0.05$, **$P < 0.01$, ***$P < 0.001$ in t-test. Data is presented as means ± SEM. (B) 3D reconstruction of the outer surface of the brains of *Zic2*$^{+/+}$ (+/+) and *Zic2*$^{kd/+}$ (kd/+) mice (gray) with lateral ventricle (green). Dorsal (left) and anterior-lateral (right) views are indicated. Note the enlarged lateral ventricles and the narrowed interspace between the left and right lateral ventricles containing septum (asterisk). (C) Morphometric analysis. Sections were subjected to acetylcholine esterase staining. (a)–(d) Lines denote the distances measured in each section (a, cerebral cortex thickness; b, corpus callosum thickness; c, medial structure rostral to the hippocampus [fimbria including septofimbrial nucleus or septal triangular nucleus]; d, subfornical organ width). The measurements were done on 15 pairs of the most comparable from the serial sections of adult male *Zic2*$^{+/+}$ and *Zic2*$^{kd/+}$ mice brains. (D) Morphometric analysis. The lengths are presented as a percentage relative to the corresponding wild-type values. *$P < 0.05$, **$P < 0.01$, ***$P < 0.001$ in t-test. Data is presented as means ± SEM. (E) Morphological abnormalities in the amygdala. The coronal sections from *Zic2*$^{+/+}$ (+/+) and *Zic2*$^{kd/+}$ (kd/+) mice were subjected to immunostaining with the anti-Zic antibody, toluidine blue (TB), and acetylcholine esterase staining (AchE). The black arrowhead and arrow indicate the Zic-positive cells in the amygdalohippocampal area (AHA) and medial nucleus, respectively. The white arrowheads indicate the enhanced AchE signals in the AHA. AMY, amygdalar complex; BLA, basolateral nucleus of amygdala; COA, cortical nucleus of amygdala; DT, dorsal thalamic nuclei; LA, lateral nucleus of amygdala; MEA, medial nucleus of amygdala; MH, medial habenular nucleus; MN, meningeal membrane. Scale bars, 0.5 mm.

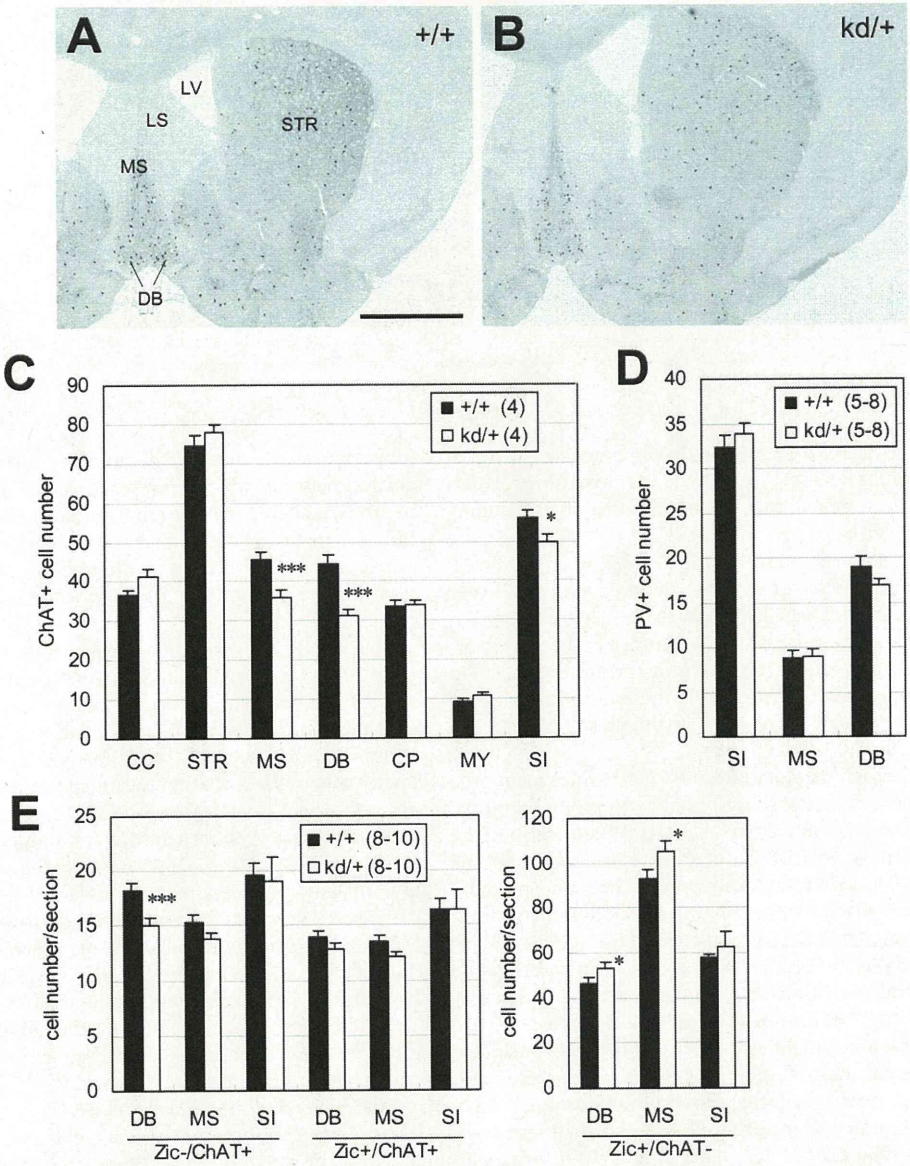

Figure 5 | Decreased number of cholinergic neurons in the brains of *Zic2*$^{kd/+}$ mice. (A,B) Immunostaining of the brains of *Zic2*$^{+/+}$ (+/+) (A) and *Zic2*$^{kd/+}$ (kd/+) (B) mice with anti-ChAT antibody. Coronal sections through the septum and diagonal bands derived from adult male mice were subjected to immunoperoxidase staining. Scale bar, 1 mm. (C) Number of the ChAT$^+$ neurons in the sections. Mean numbers of ChAT$^+$ neurons in 20 sections from the *Zic2*$^{+/+}$ and *Zic2*$^{kd/+}$ mice brains are indicated. (D) PV-positive cell numbers. The measurements were taken in comparable regions to those subjected to ChAT-immunostaining. (E) The numbers of ChAT- and Zic-immunoreactive neurons in early postnatal (P5-7) *Zic2*$^{+/+}$ and *Zic2*$^{kd/+}$ brains. Double labeling was performed with the anti-ChAT antibody and anti-pan Zic antibody. CC, cerebral cortex; CP, caudoputamen; DB, diagonal band; LV, lateral ventricle; LS, lateral septum; MS, medial septum; MY, Mynert nucleus; SI, substantia innominata; STR, striatum. (C–E) Data is presented as means ± SEM. The number of mice in each group is given in parentheses. $^*P < 0.05$, $^{***}P < 0.001$ in t-test.

Zic2. Taken together, these results suggested that the R409P mutation dampens the transcriptional activation capacity of Zic2 by altering the properties of the Zic2-containing molecular complex.

Discussion

Our behavioral analysis in mice uncovered some novel roles of Zic2 related to higher brain function. A summary of the results from this behavioral analysis and that of previous studies is provided in Table 1.

The locomotor activity differences between wild-type and *Zic2*$^{kd/+}$ mice were context-dependent. In home cages, the mutant mice showed reduced locomotor activity in the early dark phase compared to wild-type mice, but in the open field test the mutant mice showed higher locomotor activity than wild-type mice. The tendency for *Zic2*$^{kd/+}$ mice to display higher activity in a novel environment, compared to wild-type mice was also observed in the the Y-maze test and the light-dark box test (Figure S1C). Therefore, *Zic2*$^{kd/+}$ mice appear to be generally hyperactive upon exposure to a novel environment. This hyperactivity is possibly consistent with symptoms of schizophrenia in humans; hyperactivity in response to a novel environment has been suggested as a useful animal correlate of schizophrenia symptoms[34] and has been noted in some genetically engineered mouse models of schizophrenia[35–37].

We demonstrated cognitive dysfunction in *Zic2*$^{kd/+}$ mice by the water maze test, the fear-conditioning test, and the Y-maze test. In addition, abnormal PPI, which is deemed to reflect impaired

Table 2 | Allelic frequencies of non-synonymous mutations in the *ZIC2* gene in patients with schizophrenia and control subjects.

	Control				Schizophrenia				
Polymorphism	Genotype count			MAF[2]	Genotype count			MAF	Polyphen (PSIC)[1]
Ala95Thr (283G>A)	G/G	G/A	A/A	0	G/G	G/A	A/A	0.041	Benign (0.897)
	1,036	0	0		1,226	1	0		
Ins239His	del/del	del/ins	ins/ins	8.95	del/del	del/ins	ins/ins	8.77	
	865	173	7		1,025	198	9		
Arg409Pro	G/G	G/C	C/C	0	G/G	G/C	C/C	0.04	Probably damaging (2.745)
(1,226G>C)	1,058	0	0		1,238	1	0		
Ser444Arg	C/C	C/A	A/A	0.284	C/C	C/A	A/A	0.363	Possibly damaging (1.541)
(1,332C>A)	1,051	6	0		1,230	9	0		

[1]Polyphen is a computer algorithm used to predict the effects of non-synonymous single-nucleotide polymorphisms (SNPs) on protein structure and function [30]. PSIC, difference in position-specific independent counts.
[2]MAF, minor allele frequency

sensorimoter-gating function seen in schizophrenia, is reported in *Zic2*$^{kd/+}$ [12]. These results corroborate that the cognitive function deficits in *Zic2*$^{kd/+}$ mice are not simple, but multimodal ones including sensorimotor gating function.

Social behavioral abnormalities in *Zic2*$^{kd/+}$ mice were characterized by a reduction in aggressive behavior compared to the wild-type controls in the absence of clear deficits in the affiliative behaviors. The aggressivity assessed in the resident-intruder and social dominance tube tests may be related to their territory protecting behavior. The absence of depression-like behavior in these mice excludes the possibility that their reduced aggressivity was the result of a general loss in motivation.

Collectively, the behavioral phenotypes of *Zic2*$^{kd/+}$ mice seem to be implicated in the three classes of schizophrenia symptoms (positive/negative symptoms and cognitive dysfunction). When we compare the *Zic2*$^{kd/+}$ mice phenotype with those of other typical schizophrenia model mice (Table 3), novelty-induced hyperactivity and prepulse inhibition reduction were commonly found in the dominant negative DISC1 transgenic[38]and NRG1 transmembrane KO[35]and conditional KO of ErbB4 in PV-positive interneuron[39]. In addition, the enlargement of lateral ventricle and decrement of working memory were shared with *Zic2*$^{kd/+}$ and some of them (Table 3).

The morphological abnormalities in the brain of *Zic2*$^{kd/}$ include a reduction in the septal mass, thinning of the cerebral cortex and corpus callosum, narrowing of the fimbria hippocampi, and a regional reduction of amygdalar nuclei. These abnormalities have a pathophysiological resemblance to neuropsychiatric disorders in humans. In particular, enlarged lateral ventricles and decrease in whole brain volume are a symptom of the first episode of schizophrenia[16–18], and have been observed in some genetically-engineered mouse models of schizophrenia[15,37,38,40,41]. These finding add further support for the genetic involvement of *ZIC2* in the pathogenesis of schizophrenia.

Regarding the basis of neural circuits underlying the higher brain function abnormalities observed in *Zic2*$^{kd/+}$mice, we consider the following two observations to be significant. Firstly, we observed a reduction in the number of cholinergic neurons in the basal forebrain, which raises the possibility that abnormal cholinergic regulation of higher brain function underlies the behavioral abnormalities seen in *Zic2*$^{kd/+}$ mice. Basal forebrain cholinergic neurons are thought to be capable of regulating the cortical processing of sensory stimuli within various domains[42]. In addition, recent studies indicate that the cholinergic system modulates cognitive deficits in schizophrenia and that cholinergic transmission is a potential target of therapeutics for the improvement of cognitive functions[43]. Thus, further evaluation of the cholinergic transmission dynamics in *Zic2* mutants would be beneficial for a better understanding of the role of Zic2 in cognitive function. We also examined the distribution of PV-positive cells in medial and dorsolateral prefrontal cortices and in the hippocampus (Figure S3) because the distribution of PV-positive cortical neurons, which represent a subset of GABAergic inhibitory neurons, is altered in some animal models of schizophrenia[40,44] and is thought to be a key abnormality underlying the pathogenesis of schizophrenia[45]. However, we did not observe any significant alterations in the distribution of PV-positive cells in *Zic2*$^{kd/+}$ cortices (Figure S3).

Our second key observation relates to those implying that abnormalities of the amygdala underlie the social behavior abnormalities in *Zic2*$^{kd/+}$ mice. The reduced aggressivity of *Zic2*$^{kd/+}$ mice was indicative of abnormal social behavior and we hypothesized that abnormalities of the amygdala were involved for a number of reasons. Firstly, it is well known that the amygdala is essential for controlling aggressive behaviors[46]. Also, lesions in the rat medial amygdala cause a reduction in aggressive behavior[47]. Adding further support, a recent study showed that the AHA and medial amygdala project into the hypothalamic aggression area (mediobasal hypothalamus), which plays a central role in the control of aggressive behavior[48]. These facts led us to hypothesize that the reduced aggressivity in *Zic2*$^{kd/+}$ mice is related to the altered morphology of AHA. However, there have been limited studies focusing on the role of AHA in aggressive behavior. Therefore, further investigation of the amygdalar abnormalities in *Zic2*$^{kd/+}$ mice would contribute to our understanding of the neural circuits controlling aggressive behavior.

The molecular mechanism of developmental disturbances that lead to the cholinergic neuronal loss and amygdalar dysgenesis remains elusive. As one interpretation, these abnormalities may reflect a milder representation of the HPE-like abnormality[8] and cortical dysgenesis partly as a result of the abnormal *Zic2*-expressing meningeal progenitor cells[11] in *Zic2*$^{kd/kd}$ mice. In terms of forebrain cholinergic neuron development, we found that the p75-expressing cholinergic progenitor neurons in the prospective medial septum and diagonal band are missing in *Zic1*/*Zic3* compound mutant mice[49]. Since the structure and function of the vertebrate Zic family of proteins is highly conserved[3], Zic2 might function to expand the medial forebrain cholinergic neural progenitor cells by inhibiting their exit from the proliferating cell cycle in a manner analogous to that in the *Zic1*/*Zic3* compound mutant mice[49].

Resequencing analysis of *Zic2* in Japanese patients with schizophrenia revealed three novel nonsynonymous mutations in *ZIC2*. Functional analysis of these mutations in the *Zic2*$^{kd/+}$ mouse model of schizophrenia indicated that the R409P mutation results in severe loss-of-function. We showed that the transcriptional activation capacity of the Zic2-R409P protein was about 20% that of the wild-type protein; which corresponds to the decreased protein production from the *Zic2*^{kd} allele shown previously[8]. This finding in turn validates *Zic2*$^{kd/+}$ mice as an animal model of the R409P mutation in schizophrenia. The patient with the R409P mutation was diagnosed with residual-type schizophrenia.

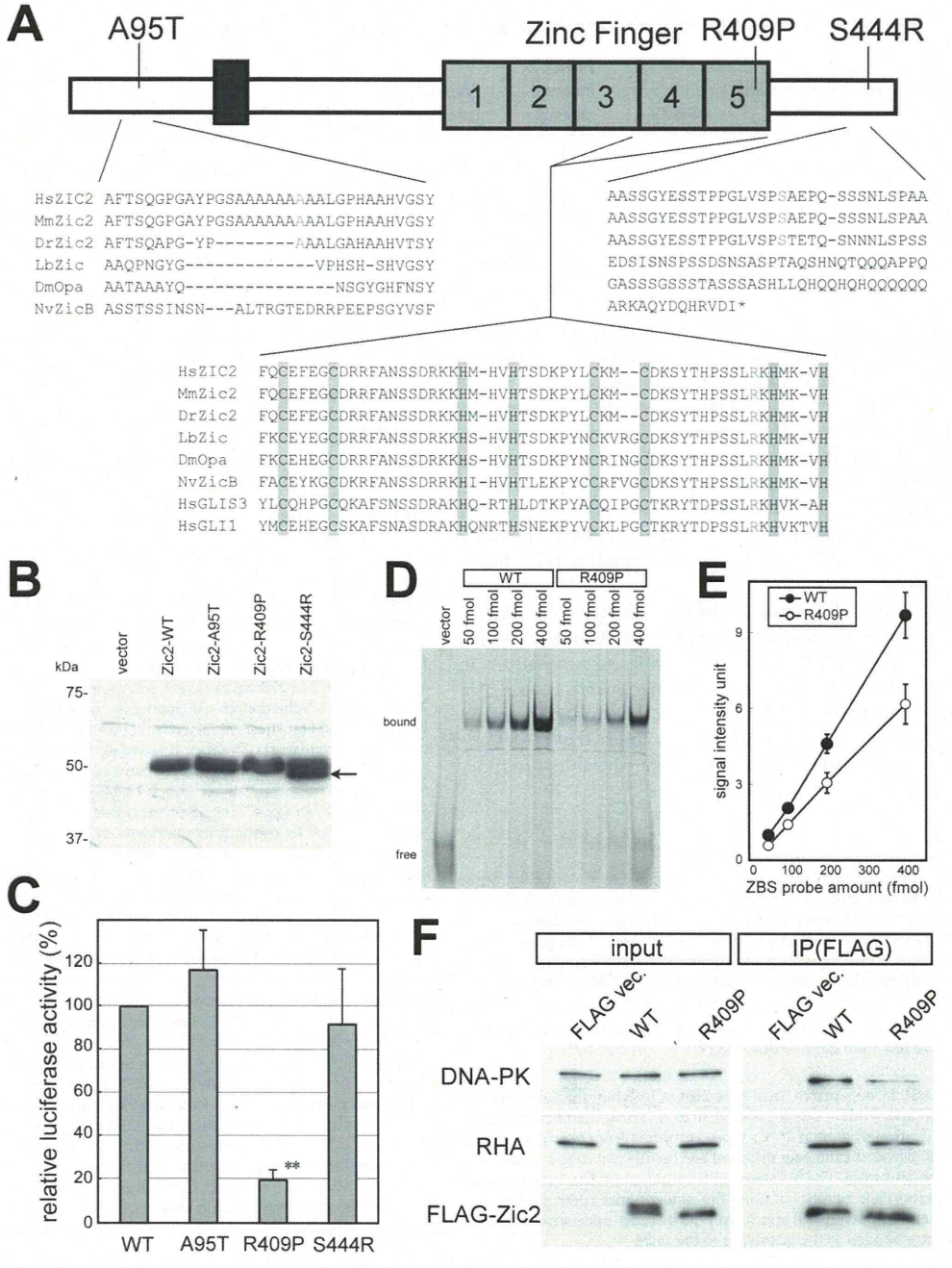

Figure 6 | Properties of ZIC2 variants found in schizophrenia patients. (A) Structure of the ZIC2 protein. Gray boxes with numbers indicate C2H2 motifs in the zinc finger domain of ZIC2. The positions of the A95T, R409P, and S444R mutations are indicated. Multiple alignments of the flanking regions of three mutations are indicated along with the reference sequences. Shaded characters show conserved cysteine and histidine residues in the C2H2 zinc fingers. Black box indicates an evolutionary conserved domain (ZOC, Zic-Opa-Conserved) domain. Gray characters indicate the mutated residues and the corresponding residues in other species (Hs, *Homo sapiens* [human]; Mm, *Mus musculus* [mouse]; Dr, *Danio rerio* [zebrafish]; Lb, *Loligo breekeri* [squid]; Dm, *Drosophila melanogaster* (fly); Nv, *Nematostella vectensis* [sea anemone]). (B) Immunoblotting of mouse wild-type Zic2 and Zic2 variants. NIH3T3 cells were transfected with the FLAG-tag expression plasmids. The Zic2 proteins were detected by the anti-FLAG antibody. Arrow indicates the fast migrating component in FLAG-Zic2-S444R. (C) NIH3T3 cells were transfected with a Zic2-responsive luciferase reporter vector together with a vector expressing wild-type FLAG-Zic2 (WT), or the FLAG-Zic2-A95T, -R409P, -S444R mutant proteins. All luciferase activities were normalized to the activities of the co-transfected elongation factor 1 promoter-driven Renilla luciferase. The means ± SEM of three independent experiments of three samples each are shown. (D) Gel mobility shift assay. IRD-labeled target DNAs were incubated with partially purified FLAG-Zic2-WT or FLAG-Zic2-R409P proteins expressed in 293T cells. The probes and the amount are indicated at the top. (E) Quantification of the gel shift assay result. Data are presented as means ± SEM. There were statistically significant differences between the FLAG-Zic2-WT and FLAG-Zic2-R409P-bound DNA probes at each dose (50 fmol, $P < 0.001$; 100 fmol, $P = 0.0022$; 200 fmol, $P = 0.012$; and 400 fmol, $P = 0.0089$). (F) FLAG-Zic2-WT or FLAG-Zic2-R409P expressed in 293T cells were immunoprecipitated with the anti-FLAG antibody. Proteins in the input cell lysates (input) and immunoprecipitates (IP) were analyzed by immunoblotting using anti-DNA-PK, anti-RHA, and anti-FLAG antibodies. There was a decrease in the amount of co-precipitated DNA-PK in FLAG-Zic2-R409P immunoprecipitates compared to those from FLAG-Zic2-WT, despite comparable amounts of FLAG-Zic2-R409P and FLAG-Zic2-WT.

Table 3 | Comparison of the morphological and behavioral features of *Zic2* kd/+ with those of other typical schizophrenia model mice.

	Lateral ventricular volume	Anxiety	Novelty induced activity	Working memory	PPI	Social recognition	R-I aggression	Social interaction
Zic2 kd/+	↑	=	↑	↓	↓	=	↓	=
DISC1-DN	↑	=	↑	=	↓	-	-	=
NRG1-TM	-	=	↑	=	↓	↓	↑	=
PV-ErbB4-/-	-	-	↑	↓	↓	-	-	-

Dominant negative *Disc* transgenic (DISC1-DN) and *Nrg1* transmembrane knockout (NRG1-TM) results summary is based on [20]. Conditional knockout of *Erbb4* in PV-positive interneuron (PV-ErbB4-/-) is based on [39]. ↑, increased relative to WT; ↓, decreased relative to WT; =, no difference; -, not reported.

Many studies have investigated the *ZIC2* mutations in patients with HPE. A recent meta-analysis study of previously published results showed that the vast majority of *ZIC2* mutations (98%) cause significant loss-of-function[7]. This suggests that HPE is caused by severely impaired function of ZIC2. Interestingly, only the very few cases (three families), in which the function of *ZIC2* was shown to be null, included two independent parents with normal brain imaging despite the identification of *ZIC2* missense mutations (Q36P or D152F)[7]. Together with these results, our findings raise the possibility that mildly impaired ZIC2 function does not result in HPE, but in psychiatric illnesses.

In summary, behavioral and morphological phenotypes in $Zic2^{kd/+}$ mice were reminiscent of those of schizophrenia. Additionally, the detection of rare, but significantly defective, missense mutations in patients with schizophrenia suggests that further analysis of *ZIC2* in neuropsychiatric patients is meaningful. Since this study focused on missense mutations, there still remains the possibility that mutations in introns and/or flanking regions that provoke partial loss of function are associated with schizophrenia.

Methods

Animals. Animal experiments were approved by the Animal Experiment Committee of the RIKEN Brain Science Institute (approval no. H22-EP068), and the mice were maintained by the institute's Research Resource Center. Mutant mice heterozygous for the $Zic2^{kd}$ allele ($Zic2^{kd/+}$) were described previously[8,9,12]. $Zic2^{kd}$ was generated by the insertion of the neomycin resistant cassette into an intron of mouse *Zic2*, resulting in the 20% of the wild-type allele[8], and were maintained in C57BL/6J background.

Behavioral tests. Home cage activity measurement, open field test, classical fear conditioning, Y-maze test were done as described[50,51].

Resident-intruder test. Group-reared mice were kept in isolation for 5 days before the test. The test was carried out in a dark phase (0:30 to 2:30) in a chamber that keeps the cage under dim (infrared) light at 25°C. Video recording from two opposite directions was initiated once the intruder mice had been gently placed in a vacant spot in the cage of the resident mice. The behaviors of the resident mouse were recorded for 10 min. The duration and number of times the resident mice spent sniffing, in active contact with, and in pursuit and attack with the intruder mice were measured by observers who were blinded to the genotypes of the mice.

Social dominance tube test. A wild type and a $Zic2^{kd/+}$ mice were placed in a head-to-head position first at the opposite ends of a clear plexiglass tube (3.4 cm inner diameter, 30 cm in length) in which two shutter plates were inserted at a distance of 13 cm from each end. The tests were begun by removing the shutters and ended when one mouse completely retreated from the tube. The mouse that retreated first was designated as the loser, and the remaining mouse was judged as the winner. The maximal test time was set to 2 min.

Magnetic resonance imaging (MRI) based volumetric analysis. MRI images of the adult male mice were acquired by subjecting anesthetized mice to an MRI scan using a vertical bore 9.4-T Bruker AVANCE 400WB imaging spectrometer (Bruker BioSpin, Rheinstetten, Germany). Animals were anesthetized with 3% and 1.5% isoflurane in air (2 L/min flow rate) for induction and maintenance, respectively. MRI images were obtained by using the FISP-3D protocol of Paravision software 5.0, by setting the following parameter values: Effective TE = 4.0 ms, TR = 8.0 ms, Flip angle = 15 degree, Average number = 5, Acquisition Matrix = 256 × 256 × 256, FOV = 25.6 × 25.6 × 25.6 mm. Manual measurements were made on the 3-dimensional (3D) MRI data to calculate total brain volume, hippocampus volume and lateral ventricle volume using the InsightITK-Snap software[52]. Regional volumetric changes were measured by voxel-based morphometry (VBM) using the Statistical Parametric Mapping (SPM) software package (http://www.fil.ion.ucl.ac.uk/spm/software/) for MATLAB (Mathworks, Natick, MA, USA) for pilot survey (data not shown).

Histology and immunostaining. Histological examination was done as described[9]. For the morphometric analysis, serial coronal sections were prepared, and analyzed at the following positions: +0.74 to +1.10 for the septum, diagonal band, striatum and the motor cortex; −0.34 to −0.82 for the substantia innominata, the basal nucleus of the Meynert, and the somatosensory cortex [anterior(+) to posterior(−) distance (mm) from bregma according to Paxinos et al.[53]]. The sections were stained with cresyl violet or by utilizing endogenous acetylcholine esterase activity[54] for histological examination.

Immunostaining was performed as previously described[55]. The primary antibodies were rabbit mouse anti-choline acetyltransferase (ChAT) polyclonal antibody (Chemicon, Temecula, CA, USA), mouse monoclonal anti-parvalbumin (PV) (Sigma, St. Louis, MO, USA), and rabbit anti-pan-Zic antibodies[10].

Resequencing analysis of *ZIC2* in human subjects. We performed resequencing analysis of *ZIC2* in 278 patients with schizophrenia who were of Japanese descent. The diagnosis of schizophrenia including the samples below was made on the basis of Diagnostic and Statistical Manual of Mental Disorders criteria (DSM-IV), by at least two expert psychiatrists. We then determined the allele frequencies of detected mutations using an expanded sample panel of schizophrenia patients (967 subjects: 457 men, 510 women; mean age 47.3 ± 13.8 [SD] years) and 1060 controls (502 men, 558 women; mean age 47.7 ± 13.6 years) who were documented as being free of mental disorders following brief interviews by expert psychiatrists. Our recruitment of schizophrenia and control subjects did not involve structured or semi-structured instruments. This study was approved by the ethics committees of RIKEN.

Protein-coding regions and exon/intron boundaries within the *ZIC2* gene were screened for polymorphisms by direct sequencing of PCR products using the BigDye Terminator v3.1 Cycle Sequencing kit (Applied Biosystems, Foster City, CA, USA) and the ABI PRISM 3730xl Genetic Analyzer (Applied Biosystems).

Molecular and functional analysis. Mouse *Zic2* variants that have the same missense mutations as the human *ZIC2* nonsynonymous mutations ($Zic2^{A95T}$ for $ZIC2^{A95T}$, $Zic2^{R408P}$ for $ZIC2^{R409P}$, and $Zic2^{S443R}$ for $ZIC2^{S444R}$) were generated by PCR[56] using pEFBOS-$Zic2^{31}$ or pcDNA3-HA-*Zic2* as templates. Hereinafter, we refer to them as *Zic2*-A95T ($Zic2^{A95T}$), *Zic2*-R409P ($Zic2^{R408P}$) and *Zic2*-S444R ($Zic2^{S443R}$), respectively. Expression plasmids for these wild-type *Zic2* and *Zic2* variants were constructed pcDNA3.1 (Invitrogen, Carlsband, CA, USA) and pCMVtag2 (Stratagene, La Jolla, CA, USA). pGL4-ZBS was constructed by inserting a mouse genomic DNA clone containing Zic2-binding sequences (Ishiguro et al., unpublished) into pGL4 (Promega, Madison, WI, USA). Cell culture, transfection, immunoblot analysis. luciferase reporter assay, gel shift assay, and immunoprecipitation were performed as previously described[31,33].

Statistical analysis. Parametric data were analyzed by using the two-sided Student's *t*-test (t-test) and non-parametric data were analyzed by using the Mann–Whitney's *U*-test (U-test). The *P* values refer to the t-test, unless otherwise specified. We also used the repeated measure two-way analysis of variance (RMANOVA) or the chi-square test for homogeneity. Differences were defined as statistically significant when $P < 0.05$.

1. Aruga, J. *et al.* The mouse zic gene family. Homologues of the Drosophila pair-rule gene odd-paired.*J Biol Chem* **271**, 1043–1047 (1996).
2. Nagai, T. *et al.* The expression of the mouse Zic1, Zic2, and Zic3 gene suggests an essential role for Zic genes in body pattern formation. *Dev Biol* **182**, 299–313 (1997).
3. Aruga, J. The role of Zic genes in neural development. *Mol Cell Neurosci* **26**, 205–221 (2004).
4. Grinberg, I. & Millen, K. J. The ZIC gene family in development and disease. *Clin Genet* **67**, 290–296, doi:10.1111/j.1399-0004.2005.00418.x (2005).
5. Merzdorf, C. S. Emerging roles for zic genes in early development. *Dev Dyn* **236**, 922–940 (2007).
6. Brown, S. A. *et al.* Holoprosencephaly due to mutations in ZIC2, a homologue of Drosophila odd-paired. *Nat Genet* **20**, 180–183 (1998).